



STUDY ON PARTIALLY SHADED CONDITIONS REGULATORS FOR PV BASED ELECTRICALLY POWERED VEHICLES

Universidade do Algarve

Instituto Superior de Engenharia

Departamento de Engenharia Elétrica e Eletrónica

Author: Élide Mendieta Irisarri (73413)

Tutor: Professor Cristiano Lourenço Cabrita

JULY 2021

ACKNOWLEDGEMENTS

I would like to express my gratitude to the director of this project, Professor Cristiano Lourenço Cabrita, for guiding me, helping me specially when I was blocked, for getting so involved in the project and dedicating so many hours to it.

I also want to thank Engineer Carlos Miguel Santos, assistant in the laboratory of Mechanical Engineering for his help and patience during the long sessions in the laboratory.

OBRIGADA

I would also thank the Erasmus+ program, my home university, Universidad Pública de Navarra and Universiade do Algarve for giving me the opportunity of studying one semester abroad.

THANKS

Special thanks to my parents, who will always be my best supporters and to my friends who have made this path more pleasant.

GRACIAS

ABSTRACT

At present times, the inclusion of renewable energies in the field of transportation has become crucial to reduce its contaminant emissions.

One way in which transportation could take advantage of solar energy is by installing photovoltaic panels on the surface of the vehicles and use their power to charge the battery of electric/hybrid vehicles.

An important condition that should be considered is the variability of the solar irradiance. If the panels are set in the surface of a vehicle, their orientations are different. Consequently, the irradiance each panel receives is different from one to another.

The department of Mechanical Engineering has 4 photovoltaic panels of around 30W maximum power each which will be studied and will serve as reference for the panels in the study, simulating they are the panels that could be set in the surface of a vehicle.

Afterwards, these panels are going to be simulated in MATLAB/Simulink forming part of a photovoltaic system with a load regulator feeding a battery under partially shaded conditions (PSC).

A maximum power point tracking (MPPT) algorithm capable of working under PSC is going to be implemented in the simulation of the system and its operation is going to be compared to the operation of a commonly used algorithm.

Key words: photovoltaic panel, DC/DC converter, load regulator, maximum power point tracking (MPPT), partially shaded conditions (PSC).

TABLE OF CONTENTS

| | | |
|-----------|--|-----------|
| 1. | INTRODUCTION..... | 1 |
| 2. | OBJECTIVES..... | 2 |
| 3. | STATE OF ART..... | 2 |
| 4. | THEORETICAL RESEARCH..... | 3 |
| 4.1 | CHARACTERIZATION OF THE I-V CURVE OF SOLAR PANELS | 3 |
| 4.1.1 | CHARACTERISTIC EQUATION I-V | 3 |
| 4.1.2 | CHARACTERISTIC CURVE I-V | 4 |
| 4.2 | POWER CONVERTERS AND MPPT..... | 5 |
| 4.2.1 | TYPES OF DC-DC CONVERTERS AND THEIR MANAGEMENT OF LOAD POWER | 5 |
| 4.2.2 | METHODS FOR MPPT..... | 6 |
| 5. | DEVELOPMENT..... | 11 |
| 5.1 | EXPERIMENTAL PROCEDURE FOR I-V AND P-V CURVES CHARACTERIZATION. 12 | |
| 5.2 | SELECTION OF THE MOST ADEQUATE DC-DC CONVERTER..... | 14 |
| 5.3 | CONNECTION OF THE PV-PANELS TO A COMMERCIAL LOAD REGULATOR..... | 14 |
| 5.4 | BOOST CONVERTER PROVIDING A CONSTANT OUTPUT VOLTAGE..... | 16 |
| 5.4.1 | DIMENSIONING OF THE BOOST CONVERTER | 16 |
| 5.4.2 | ALGORITHM FOR TRACKING THE OUTPUT VOLTAGE | 18 |
| 5.5 | LOAD REGULATOR WITH MPPT ALGORITHMS..... | 18 |
| 5.5.1 | MODEL OF THE PHOVOVOLTAIC ARRAY..... | 19 |
| 5.5.2 | MODEL OF THE COMPLETE SYSTEM..... | 20 |
| 5.5.3 | PERTURBATION AND OBSERVATION ALGORITHM..... | 21 |
| 5.5.4 | DUTY SWEEPING ALGORITHM | 21 |
| 6. | RESULTS..... | 22 |
| 6.1 | CHARACTERISTIC CURVES OF THE PANELS | 23 |
| 6.1.1 | POWER-VOLTAGE CURVES OF THE PANELS | 25 |
| 6.1.2 | BEHAVIOUR OF THE P-V PANELS UNDER PARTIALLY SHADED CONDITIONS..... | 28 |
| 6.1.3 | EFFECT OF AMBIENT TEMPERATURE ON THE CHARACTERISTIC CURVE..... | 30 |
| 6.2 | VERIFICATION OF THE OPERATION OF THE COMMERCIAL LOAD REGULATOR | 31 |
| 6.3 | SIMMULATION OF THE BOOST CONVERTER FEEDING A LOAD WITH CONSTANT VOLTAGE WHILE TRACKING THE OUTPUT VOLTAGE..... | 33 |
| 6.4 | SIMULATION OF THE BOOST CONVERTER TO CARRY OUT MPPT UNDER PARTIALLY SHADED CONDITIONS | 41 |
| 6.4.1 | SIMULATION WITH PERTURBATION AND OBSERVATION ALGORITHM..... | 42 |
| 6.4.2 | SIMULATION WITH DUTY SWEEPING ALGORITHM..... | 44 |
| 7. | CONCLUSIONS..... | 46 |

| | |
|--|-----------|
| 8. BIBLIOGRAPHY AND REFERENCES..... | 50 |
| APPENDIX..... | 52 |

LIST OF TABLES

| | |
|--|-----------|
| <i>Table 4.1: Example of a fuzzy control table adapted from [9].....</i> | <i>9</i> |
| <i>Table 6.1: Maximum power extracted.....</i> | <i>27</i> |
| <i>Table 6.2: frequencies of the simulations.....</i> | <i>38</i> |
| <i>Table A.1: data recorded for panel A.....</i> | <i>52</i> |
| <i>Table A.2: data recorded for panel B.....</i> | <i>55</i> |
| <i>Table A.3: data recorded for panel C.....</i> | <i>57</i> |
| <i>Table A.4: data recorded for panel D.....</i> | <i>59</i> |
| <i>Table A.5: data recorded for array A-D under PSC.....</i> | <i>61</i> |
| <i>Table A.6: Measurements from the commercial load regulator.....</i> | <i>63</i> |
| <i>Table A.7: data recorded for panel A at high temperature.....</i> | <i>68</i> |
| <i>Table A.8: Irradiance-Current ratio for panel A.....</i> | <i>72</i> |
| <i>Table A.9: Irradiance-Current ratio for panel B.....</i> | <i>72</i> |
| <i>Table A.10: Irradiance-Current ratio for panel C.....</i> | <i>73</i> |
| <i>Table A.11: Irradiance-Current ratio for panel D.....</i> | <i>73</i> |
| <i>Table A.12: Linear factor between currents and irradiances for panel A.....</i> | <i>74</i> |
| <i>Table A.13: Linear factor between currents and irradiances for panel B.....</i> | <i>75</i> |
| <i>Table A.14: Linear factor between currents and irradiances for panel C.....</i> | <i>75</i> |
| <i>Table A.15: Linear factor between currents and irradiances for panel D.....</i> | <i>75</i> |

LIST OF FIGURES

| | |
|---|-----------|
| <i>Figure 1.1: Evolution of greenhouse gas emissions by transport in the EU [1].....</i> | <i>1</i> |
| <i>Figure 4.1: Equivalent circuit of a solar panel [5].....</i> | <i>3</i> |
| <i>Figure 4.2: Characteristic curves I-V and P-V of a solar panel under uniform irradiance.....</i> | <i>4</i> |
| <i>Figure 4.3: Characteristic curves I-V and P-V of a solar panel under PSC.....</i> | <i>4</i> |
| <i>Figure 4.4: linear relation between V_{MPP} and V_{OC}.....</i> | <i>8</i> |
| <i>Figure 4.5: Schematic diagram of the DS method presented in [3].....</i> | <i>11</i> |
| <i>Figure 5.1: schematic of the measurements.....</i> | <i>13</i> |
| <i>Figure 5.2: Image of the experimental set up.....</i> | <i>13</i> |
| <i>Figure 5.3: Boost converter connecting a PV array and a load.....</i> | <i>16</i> |
| <i>Figure 5.4: I-V and P-V curve of the array under PSC and 25°C.....</i> | <i>19</i> |
| <i>Figure 5.5: model of the system used in Simulink.....</i> | <i>20</i> |
| <i>Figure 5.6: Perturbation & Observation method.....</i> | <i>21</i> |
| <i>Figure 5.7: Duty Sweeping method.....</i> | <i>22</i> |

| | |
|--|----|
| Figure 6.1: I-V curve for panel A at 18°C..... | 23 |
| Figure 6.2: I-V curve for panel B at 18°C..... | 24 |
| Figure 6.3: I-V curve for panel C at 18°C..... | 24 |
| Figure 6.4: I-V curve for panel D at 18°C..... | 25 |
| Figure 6.5: P-V curves for panel A..... | 25 |
| Figure 6.6: P-V curves for panel B..... | 26 |
| Figure 6.7: P-V curves for panel C..... | 26 |
| Figure 6.8: P-V curves for panel D..... | 27 |
| Figure 6.9: Theoretical I-V and P-V curves under PSC obtained in MATLAB/Simulink..... | 29 |
| Figure 6.10: I-V curve obtained experimentally under PSC..... | 29 |
| Figure 6.11: P-V curve obtained experimentally under PSC..... | 30 |
| Figure 6.12: I-V curve for panel A at 24°C..... | 31 |
| Figure 6.13: Simulation with one panel feeding the load with an irradiance of 1000W/m ² | 33 |
| Figure 6.14: Simulation with 2 panels in series feeding the load with an irradiance of 1000W/m ² | 34 |
| Figure 6.15: Verification for a load of 40 Ω..... | 35 |
| Figure 6.16: Simulation with 2 strings of 2 panels in series with a variable irradiance and ΔD=0.01.... | 37 |
| Figure 6.17: Simulation with 2 strings of 2 panels in series with a variable irradiance and ΔD=0.1..... | 37 |
| Figure 6.18: Simulation with 1KHz and 200Hz..... | 38 |
| Figure 6.19: Simulation with 1KHz and 500Hz..... | 39 |
| Figure 6.20: Simulation with 20KHz and 500Hz..... | 39 |
| Figure 6.21: Simulation with 20KHz and 100Hz..... | 40 |
| Figure 6.22: Time required for a stable response..... | 41 |
| Figure 6.23: Characteristic curves of the simulated array under PSC..... | 42 |
| Figure 6.24: Simulation of P&O algorithm with initial D=0.95..... | 43 |
| Figure 6.25: Simulation of P&O algorithm with initial D=0.5..... | 43 |
| Figure 6.26: Simulation of Duty Sweeping algorithm..... | 44 |
| Figure 6.27: Simulation of Duty Sweeping algorithm with a change in irradiance..... | 45 |
| | |
| Figure A.2: Approximated I-V curves for panel A..... | 70 |
| Figure A.3: Approximated I-V curves for panel B..... | 71 |
| Figure A.4: Approximated I-V curves for panel C..... | 71 |
| Figure A.5: Approximated I-V curves for panel D..... | 72 |

1. INTRODUCTION

Transport is responsible for the consumption of one third of the total final energy in the European Union. It strongly contributes to the climate change and, as the energy used comes mostly from petrol, transport contributes to the emissions of greenhouse gases to the atmosphere. Even though the contamination due to transport has been controlled in the European Union in the last decade due to the policies established, the concentration of contaminants continues being unacceptable. It is for that reason that a transition towards low carbon-modes and zero-emission vehicles must be carried out by means of electrification and taking benefit of renewable energies [1].

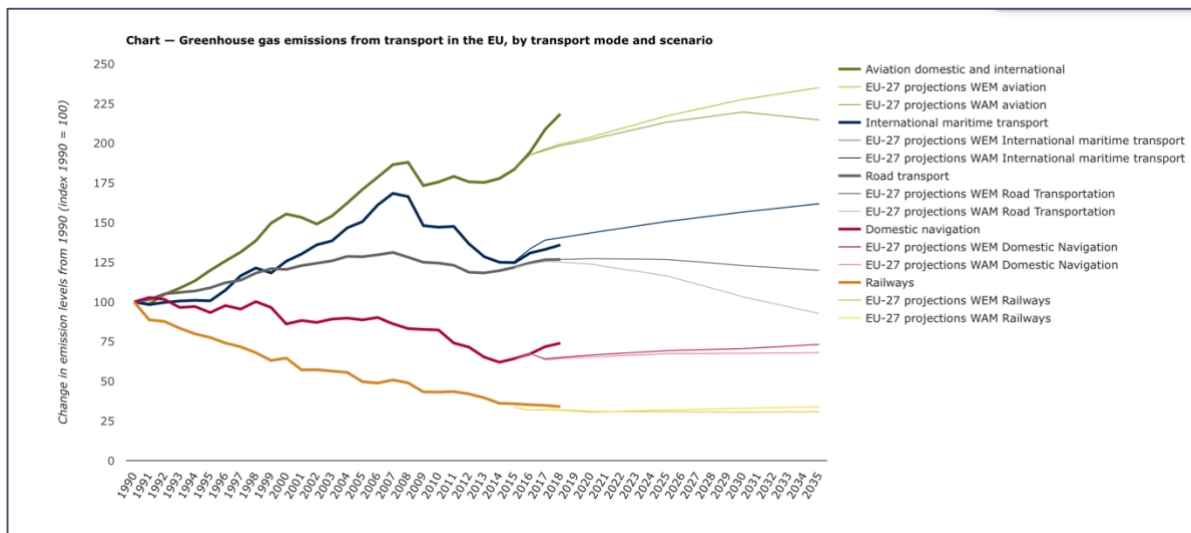


Figure 1.1: Evolution of greenhouse gas emissions by transport in the EU [1]

In the last years, the motor vehicle industry has partially moved to the design of both electric and hybrid cars. However, the main problem arises with the storage of the energy inside vehicles, mainly with the autonomy and durability of the batteries and the time required for recharging.

Although vehicles powered 100% with photovoltaic energy directly from solar panels are not common yet, the addition of panels to their surface can be a way of charging their batteries. By covering the bodywork of an electric automobile (or any other vehicle) with solar panels, its autonomy can be extended.

2. OBJECTIVES

The aim of this project is to study and simulate a solar power system connected to a DC-DC converter system, including a MPPT algorithm, to control and regulate the power supplied to a battery connected to the mentioned system.

In a more detailed way, the objectives of the present project are the following:

- Compare the different types of DC-DC converters that can be used as load regulators and compare different methods to carry out the tracking of the maximum power point.
- Study 4 monocrystalline photovoltaic (P-V) panels, measure their characteristic parameters and deduce their characteristic curve for different irradiance values.
- Simulate a DC-DC power converter connected to a photovoltaic array formed by the previously mentioned panels, dimension its components and understand its operation under different conditions of irradiance.
- Design a MPPT algorithm capable of working under partially shaded conditions and implement it on the power converter simulation.
- Compare the operation of the load regulator with the designed MPPT algorithm to its operation with a commonly used algorithm.

3. STATE OF ART

The technological context in which this project is englobed, is the field of power electronics. This is a field in which electricity and electronics are mixed, as the fine control from electronics is applied to control the opening and closing of semiconductors to carry out energy transformations from one form of electric energy to another [2].

The paper ‘Design and Implementation of a Hybrid Maximum Power Point Tracker in Solar Power System under Partially Shaded Conditions’ by Cheng-Yu Tang, Shih-Hsun Lin and Sheng-Yuan Ou is taken as a starting point for this project [3] as it proposes a hybrid MPPT method to extract the maximum power under partially shaded conditions (PSC).

4. THEORETICAL RESEARCH

In this section, the most important concepts necessary for the understanding of the project are summarized.

4.1 CHARACTERIZATION OF THE I-V CURVE OF SOLAR PANELS

The functioning principle of solar cells is based on the photovoltaic effect. Solar cells are made of semiconductive materials, which allow the circulation of electrons when a particular amount of energy is applied. The most common material is Silicon, both monocrystalline and polycrystalline are used in a similar percentage. The four solar panels under study in the present work are monocrystalline. This type of Silicon provides higher efficiency although it has a superior price [4].

4.1.1 CHARACTERISTIC EQUATION I-V

The mentioned photovoltaic effect occurs as follows: the photons from the Sun's irradiance fall upon the semiconductors, transmitting their energy to the electrons in the material and allowing them to circulate outside of the metallic contacts in the cell. Depending on the voltage at the output of the cells, the number of electrons circulating to the exterior varies. As voltage increases, the number of circulating electrons -and consequently, the current- decreases.

The characteristic equation of the solar cell defines this behavior and has the following form [5]:

$$I = I_{PV} - I_0 \left\{ \exp \left(\frac{V + IR_s}{a \cdot V_T} \right) - 1 \right\} - \frac{V + IR_s}{R_{sh}} \quad (eq. 1)$$

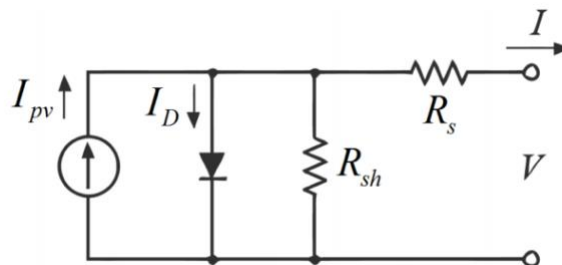


Figure 4.1: Equivalent circuit of a solar panel [5]

4.1.2 CHARACTERISTIC CURVE I-V

The representation of the characteristic equation with voltage in the x-axis and the current (and power) in the y-axis results in the characteristic curve of a solar panel. The general form that they usually have when the irradiance is uniform in the whole panel or array is the following:

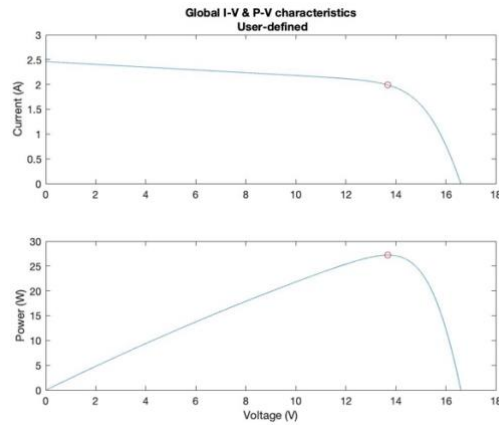


Figure 4.2: Characteristic curves I-V and P-V of a solar panel under uniform irradiance

Irradiance affects mainly to the current extracted from the panel and the short-circuit current varies almost proportional to irradiance. On the other hand, temperature has a greater effect on the voltage output of the panel. Although its effect over voltage is not as notorious as the effects of irradiance over current, the open-circuit voltage is reduced as temperature increases [4].

In the case of having one part or several parts of the panel or array shaded -that is, receiving a different value of irradiance- the characteristic curves are modified, and they take a form like the next one, presenting peaks of power along the characteristic curve.

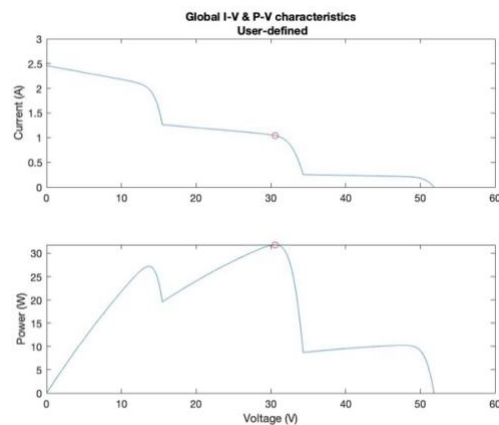


Figure 4.3: Characteristic curves I-V and P-V of a solar panel under PSC

4.2 POWER CONVERTERS AND MPPT

A power converter is a device capable of converting electric energy in one form to another. They consist of a series of semiconductors (MOSFETs, IGBTs, diodes...) used as switches together with some passive elements which act as filters for the electric signal.

In order to transform the electrical wave from one form to another, Pulse Width Modulation (PWM) is used. In this technique, the duty cycle of the switches' control signal (sinusoidal or square) is modified to get the desired electric signal at the output of the converter. The duty cycle of the control signal is the ratio between the pulse width (or time duration at which the function is positive (τ)) and the period of the signal (T):

$$D = \frac{\tau}{T} \quad (\text{eq. 2})$$

The control circuit consists of a (1) regulator (mathematical function usually) which determines the value of the control voltage ($V_{control}$); the (2) PWM modulator which calculates the control function of the switches based on the control voltage, and the (3) driver, responsible for adjusting the control function to the needs of the switches.

4.2.1 TYPES OF DC-DC CONVERTERS AND THEIR MANAGEMENT OF LOAD POWER

For the scope of this project, the converter will be of DC-DC type, as they are the most adequate for conducting MPPT and the objective is to use it to feed a battery.

As stated in [6], there is not a theory to guide the selection of the most adequate DC-DC converter and the most common ones are: Buck, Boost, Buck-Boost, Cúk, Sepic and Zeta.

As mentioned previously, power converters vary the output voltage by modifying the duty cycle (D). Even though D can theoretically take any value between 0 and 1, there are some limitations which compromise the operation of the converter. As shown in the study carried out in [6], not all the topologies can work at any cycle.

Buck-Boost, Cúk, Sepic and Zeta converters do not have any limitation, whereas Buck and Boost converters do have. In any case, although Buck and Boost converters may not have the greatest operation zone, they may be more convenient due to their simplicity of design and building.

The paper [7] also analyses the convenience of Buck and Boost converters from another point of view, the one of efficiency. The results are highly conclusive, the energetic efficiency of Boost converters is higher (around 90%) for the whole working range of the converter whereas Buck converter is only efficient when working at considerably high duty cycles.

4.2.2 METHODS FOR MPPT

There is a large variety of MPPT techniques that can be applied to the search maximum power in a P-V system. Some of the most common ones are the following:

HILL CLIMBING/PERTURBATION AND OBSERVATION (P&O)

One of the most well-known MPPT methods is the P&O method which consists in modifying the operation voltage of the P-V system [8]. On the other hand, hill climbing method involves modifying the duty cycle of the power converter. Nonetheless, these two methods are the same in reality as usually PV arrays are connected to a power converter and the way of modifying the operating voltage of the array is modifying the duty cycle of the converter.

In order to apply these MPPT algorithms, the P-V curve of the photovoltaic system is used: a small perturbation (i. e. an increment) is applied to the voltage; then, if power increases, another increment in voltage is applied. Yet, if an increment in voltage supposes a decrease in power, next, a decrement in voltage is applied. This process is repeated until the maximum power point is reached, where the system keeps oscillating around.

This method requires two sensors (voltage and current) to calculate the output voltage and is quite simple to implement. Moreover, it is not dependent of the specific P-V system under analysis, and it can be implemented analogic and digitally.

The major disadvantage of P&O methodology is the time required to reach the maximum power and the possible power losses [5,8].

Another drawback of this method is that its operation is conditioned when working under PSC. As seen in *figure 4.3*, when the PV-panels in the array receive different irradiances, the P-V curve has different local MPP. Depending on which point of the curve the perturbations are started, one maximum or another is reached. If the system reaches a maximum which is not the absolute one, the algorithm keeps oscillating around it and it does not provide the real maximum power available in the array [9].

INCREMENTAL CONDUCTANCE

This method is based on the fact that the slope of the P-V curve at the maximum power point is zero, positive on the left of that point and negative on the right of that point. As power can be expressed in terms of voltage and current and conductance consists in:

$$G = \frac{I}{V} \quad (\text{eq. 3})$$

Making some simplifications, the known as *IncCond* algorithm is deduced and the MPP can be reached by comparing the instantaneous conductance ($G = I/V$) with the incremental conductance ($\Delta I/\Delta V$).

The incremental conductance will be:

$$\Delta I/\Delta V = -I/V \quad \text{at MPP.}$$

$$\Delta I/\Delta V > -I/V \quad \text{left of MPP.}$$

$$\Delta I/\Delta V < -I/V \quad \text{right of MPP.}$$

Then, the procedure is similar to the one at P&O method, the operating point is varied by perturbations until the MPP is reached and the system keeps oscillating around it until a major change in the ambient conditions occurs and the MPP is lost [8].

For this method, two sensors (voltage and current) are also required and the true MPP is tracked. However, *IncCond* algorithms are more difficult to implement.

FRACTIONAL OPEN-CIRCUIT VOLTAGE

As the relationship between V_{MPPT} and V_{oc} is practically linear for any value of the irradiance, by previously determining the constant of proportionality k_1 , the MPP can be tracked:

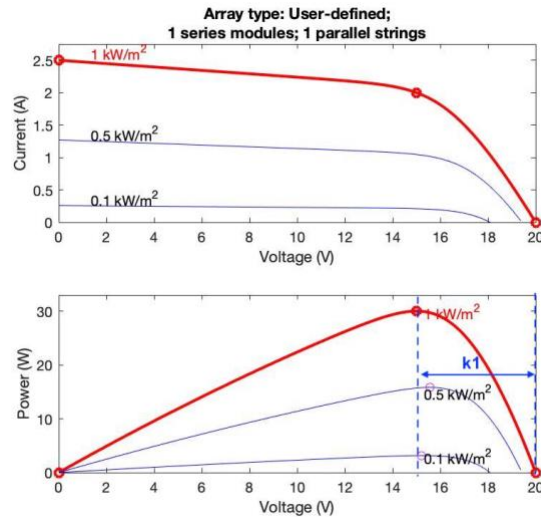


Figure 4.4: linear relation between V_{MPP} and V_{oc}

$$V_{MPP} \approx k_1 \cdot V_{OC} \quad (eq. 4)$$

Although, this method seems quite simple, as it only requires the measurement of the open-circuit voltage, it has many drawbacks. Firstly, in order to measure V_{oc} , the converter must be shutting, which implies losses of power. Secondly, as the equation characterizing this method is an approximation, the MPP reached is also approximate, it is not necessary the real one. Thirdly, the usage of the linear approximation is not valid for PSC as several maxima are found in this case [8].

FRACTIONAL SHORT-CIRCUIT CURRENT

When variable ambient conditions take place, the relation between the current at the MPP (I_{MPP}) and the short-circuit current (I_{sc}); similar to V_{MPPT} and V_{oc} (although this relation is not valid under PSC), is given as:

$$I_{MPP} = k_2 \cdot I_{SC} \quad (eq. 5)$$

The proportionality factor k_2 must also be calculated for each particular P-V array and to guaranty that MPP is being correctly tracked, it must be periodically updated.

Although a single current sensor is required, the measurement of I_{sc} is critical, the P-V system must be continuously shorted, making more components necessary.

FUZZY LOGIC CONTROL

Another way of controlling MPPT that has been introduced and works for the case of imprecise inputs in microcontrollers. These inputs are usually a variable E and a change in the error of this variable (ΔE) and they are converted into a linguistic value according to several levels. Depending on the level of the inputs, another linguistic value is given to the output (ΔD), which later is transformed in a numerical value.

An example is proposed in [9]:

The five possible levels given to the inputs are: NB (negative big), NS (negative small), ZO (zero), PS (positive small) and PB (positive big). Depending on the combination of the inputs, the output level is determined, as shown next:

Table 4.1: Example of a fuzzy control table adapted from [9]

| $E \backslash \Delta E$ | NB | NS | ZO | PS | PB |
|-------------------------|----|----|----|----|----|
| NB | ZO | ZO | NB | NB | NB |
| NS | ZO | ZO | NS | NS | NS |
| ZO | NS | ZO | ZO | ZO | PS |
| PS | PS | PS | PS | ZO | ZO |
| PB | PB | PB | PB | ZO | ZO |

As an example control rule in previous table:

If E is PB and ΔE is ZO then ΔD is PB.

This MPPT method is very convenient under variable whether conditions although it requires expertise on the field of logic control [8].

NEURAL NETWORK

Similarly to fuzzy logic control techniques, this method consists on defining a series of layers with a series of nodes in each one. The output is usually a reference, and the inputs can be the variables that the user decides but the determination of the number of layers

and the number of nodes that constitute the neural network requires expert information or, alternatively the usage of a global search-based algorithm. Depending on the inputs fed to the network and the algorithms used for adapting the parameters in the layers, the reference output is determined.

This method is very complex and requires the testing of the panels over a long period of time (eventually months) in order to reach a reliable MPPT and many parameters have to be set in the microcontroller [8].

LOAD CURRENT/LOAD VOLTAGE MAXIMIZATION

The objective of a P-V system is to feed a load with the maximum power available and this is carried out through a power converter. As the power in the load is desired to be the maximum, so will be the power at the input of the converter, and consequently the power of the load can be used as a variable for the MPPT system.

As the most usual loads connected to P-V arrays are batteries and they can be considered voltage-source type loads, only one single variable (current) is needed to be measured in order to determine MPP [10].

The main disadvantage of this method is that the real MPP is rarely achieved as the power converter is supposed to be ideal, without losses [8].

MPPT METHOD FOR PARTIALLY SHADED CONDITIONS

The methods mentioned above, are designed to follow the maximum power point under conditions of constant irradiance throughout the whole PV array. However, to operate under partially shaded conditions, they may not be capable of extracting the maximum power as they may reach a local maximum power point of the P-V curve but not the absolute power maximum (*see figure 4.3*).

The method described in the paper '*Design and Implementation of a Hybrid Maximum Power Point Tracker in Solar Power System under Partially Shaded Conditions*' ([3]) consists in an adaptation of the classical P&O method so that it can also work under PSC and reach the real maximum power point (RMPP) instead of the unique maximum power point when conditions are the same for the whole photovoltaic array.

This procedure has been called the Duty Sweep (DS) algorithm and consists in the following: the PWM of the DC-DC converter is used to vary the duty cycle (D) with a constant interval analyzing the P-V curve of the photovoltaic array which may contain one single MPP (constant irradiance conditions) or various local maxima (under PSC). Then, the power output for each of these measurements is estimated and recorded. Afterwards, once the whole range of possible D's has been scanned, the recorded power values are compared and the D corresponding to the maximum stored value is calculated and set as working parameter of the converter. Finally, classical P&O method is applied to ensure the duty cycle keeps being the corresponding one to MPP. This procedure is constantly applied so that the duty cycle of the converter is, at any moment, the one corresponding to the maximum power output.

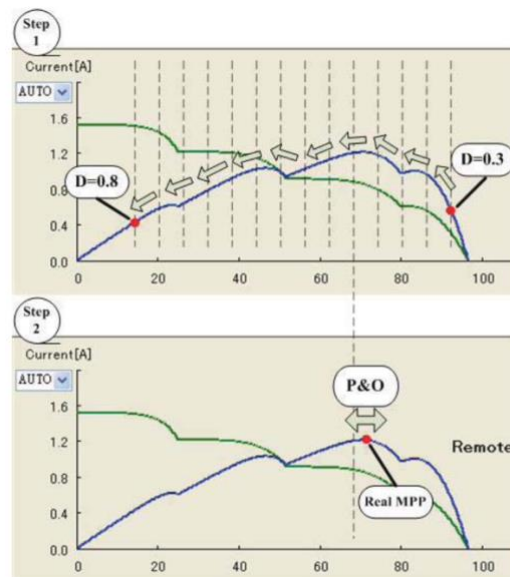


Figure 4.5: Schematic diagram of the DS method presented in [3]

5. DEVELOPMENT

The development of this project consists of 3 parts:

The first one, carrying out an experimental procedure for characterizing the working parameters of the set of 4 PV-panels available in the Mechanical Engineering Laboratory.

The second one, studying the behavior of a commercial load regulator available at the Mechanical Engineering department.

The third one, simulating in MATLAB/Simulink a system formed by some of these panels (representing their characteristics on a Simulink model) connected to a load regulator feeding a battery and being controlled by different algorithms to observe the differences in their operation.

5.1 EXPERIMENTAL PROCEDURE FOR I-V AND P-V CURVES CHARACTERIZATION

To define the working parameters of the panels their characteristic curve is going to be experimentally deduced and the following procedure of measuring is carried out for each of the panels individually:

Each panel is set at different orientations, which supposes a different irradiance for each of the settings. At each of these situations, the characteristic curve of the panel is studied:

- The **irradiance** that reaches the panels is measured with a pyranometer. This device gauges both the total and diffuse irradiance received by the panels. For the measurements, it is located next to the panels, with the same orientation as them. In order to study the effect of different irradiance values, the measurements are carried out in different days and in different orientations with respect to the Sun. By these circumstances, the different values of irradiance reaching the surface of a vehicle are simulated.
- The **ambient temperature** is measured at the meteorological station located at the *Instituto Superior de Engenharia* of the *Universidade do Algarve*.
- The **surface temperature** of the panels is measured with a thermocouple, located at the back surface of each panel.
- The **short-circuit current** and **open-circuit voltage** (extrema points of the I-V curve) are measured for each irradiance as well as **other I-V points in the curve**. In order to measure these other points of the curves, one rheostat (variable resistor)

of maximum $20\ \Omega$ and a resistor of $20\ \Omega$ are used. The combination of these two devices provides a range of resistance from 0 to $40\ \Omega$ (in intervals of $2\ \Omega$), which allows the study of the range of output currents. First, only the rheostat was connected (range from 0 to $20\ \Omega$) and later, the resistor was connected in series to continue the range from 20 to $40\ \Omega$.

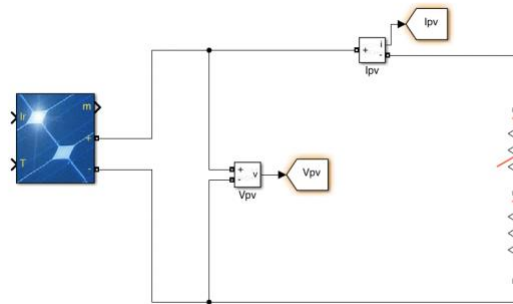


Figure 5.1: schematic of the measurements

By measuring the output current and voltage for different values of the resistor, the characteristic curve can be completely defined.



Figure 5.2: Image of the experimental set up

This procedure is repeated during several days to study the behavior of the panels with different ambient temperatures and a wide range of irradiance values.

To characterize a curve under partially shaded conditions, an array of two panels in series is set with one receiving direct irradiance from the sun and the other receiving

no irradiance. Panel D is set with an inclination of 45° with respect to the ground facing the sun while panel A is covered.

The procedure for measuring the voltage and current is the same as in the previous procedure but to study the array composed of two panels, a higher resistance is needed. For that purpose, a rheostat of 1000Ω is combined in series and in parallel with the rheostat and resistance used in previous measurements.

The experimental results of the measurements carried out at the working field can be found in *APPENDIX 1*.

5.2 SELECTION OF THE MOST ADEQUATE DC-DC CONVERTER

After having analyzed the different converters, it has been decided to implement a Boost converter due to its simplicity (compared to Buck-Boost, Cúk, Sepic and Zeta) and due to the battery, which will be used in the simulations (compared to Buck).

The battery which is going to be implemented in the simulation is one of 72V like the ones commonly used in electric vehicles like scooters. And, as the panels will be set, in arrays of maximum two panels to properly see the PSC effects, the voltage at their output will be smaller than the voltage of the battery. Consequently, a Boost converter is required to elevate the voltage in the input to the level of the output instead of a Buck which would reduce the voltage at the input.

The value of the duty cycle in a boost converter is given by [2]:

$$V_{load} = \frac{1}{1-D} \cdot V_{module} \quad (eq. 6)$$

5.3 CONNECTION OF THE PV-PANELS TO A COMMERCIAL LOAD REGULATOR

The final objective of this project is to design and simulate a load regulator that maximizes the power extracted from the solar panels at each moment. Hence, to design it, it is interesting to see how a real load regulator operates.

A commercial load regulator is connected to the P-V panels available in the university. The model used for these measurements is *Solarix medium* from *Steca* which has the following specifications:

- Maximum input current: 8 A.
- Maximum output current: 16 A.

The input of the load regulator is connected to the system of P-V panels and the output is connected to a luminous resistance (6.6Ω). The regulator is also connected to a set of 2 batteries (12V each) connected in series (24V), from the model *Tudor TC900 90Ah 720 A*.

In order to see the functioning of the mentioned load regulator, different configurations of the panels are connected to its input and the voltage and current at the input, at the load and at the batteries are measured.

The different configurations used to study the functioning of the P-V array together with the load regulator are the following ones:

- CONFIGURATION 1: the panels facing the Sun with an inclination of 45° with respect to the ground arranged in two strings connected in parallel. That is: panel A in series with panel B forming the first string, panel C in series with panel D forming the second string and these two strings connected in parallel with the load regulator.
- CONFIGURATION 2: the same configuration as 1, but with the first string (A in series with B) being shaded.
- CONFIGURATION 3: the initial configuration with one panel from each string shaded (A in the first string and C in the second).
- CONFIGURATION 4: only the string formed by A and B facing the sun with an inclination of 45° with respect to the ground.

After carrying out the measurements, the results obtained for the different configurations are presented in *APPENDIX 2*.

5.4 BOOST CONVERTER PROVIDING A CONSTANT OUTPUT VOLTAGE

The final objective of this project is to design a load regulator that provides the maximum power available in the PV-array at every moment. However, in a first approach for dimensioning the elements of the converter, a PV system feeding a load with a constant voltage will be simulated.

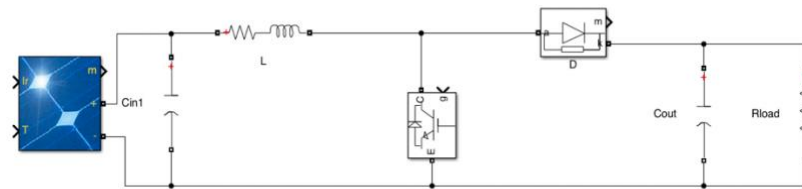


Figure 5.3: Boost converter connecting a PV array and a load

The Boost converter is composed of 4 elements, the (1) inductor, (2) the electronic switch which can consist of a MOSFET, an IGBT or a BJT (IGBT in this case), (3) the diode and (4) the output capacitor. Nevertheless, as the input of this converter is a PV array and the switch is going to impose a current at the input of the converter, a capacitor (C_{in}) must be included between the array and the input of the converter. Furthermore, this capacitor will influence the transient voltage of the array.

5.4.1 DIMENSIONING OF THE BOOST CONVERTER

The desired output voltage is set to 24 V as the battery used in the study of the commercial load regulator was a 24V battery and the first simulation is carried out with a single panel at 25°C and an irradiance of 1000W/m² having approximately the same characteristic curve as the panels studied in the laboratory. As a consequence, it is known that the maximum power parameters are the following:

$$P_{\max} = 30 \text{ W} \quad V_{MPP} = 15 \text{ V} \quad I_{MPP} = 2 \text{ A}$$

As the maximum power transferable is 30W and the output voltage is 24V, the resistance should have a minimum value of 19.2Ω:

$$P_{max} = V(P_{max}) \cdot I(P_{max}) = \frac{V(P_{max})^2}{R} \quad (eq. 7)$$

$$R = \frac{V(P_{max})^2}{P_{max}} = \frac{24^2}{30} = 19.2\Omega \quad (eq. 8)$$

To set a bit of margin, the resistance used in the simulation will have 20Ω (consequently its power requirement will be 28.8W). The switching frequency of the pulse generator is set to 10kHz.

Based on these parameters, the components of the regulator are calculated:

As *eq.6* states, the expected duty cycle when the input voltage is 15V and the output voltage is 24 is:

$$D = 1 - \frac{V_{module}}{V_{load}} = 1 - \frac{15}{24} = 0.375 \quad (eq. 9)$$

The value of the minimum inductance is calculated to ensure that the system works under continuous conduction mode (CCM) and that the current at the inductor never reaches zero because, if discontinuous conduction mode (DCM) is achieved, the relation between the duty cycle and the voltages at the input and the output stated in *eq.6* will no longer hold and a different behavior of the converter would appear [11]:

$$L_{min} = \frac{(1-D_{crit})^2 \cdot D_{crit} \cdot R_{load}}{2 \cdot f} = 0.125mH \quad (eq. 10)$$

(Being $D_{crit}=0.5$ as it is the value for which the expression is maximum.)

In order to ensure that DCM is not achieved, a margin is considered, and L is set to be $L = 0.5mH$.

The value of the minimum output capacitance is calculated according to the maximum ripple desired at the output and a common limit used is a ripple of 1% [2]:

$$C_{out min} = \frac{D}{R \cdot f \cdot \Delta V_{load}} = \frac{0.375}{20 \cdot 10000 \cdot 0.01} = 0.188mF \quad (eq. 11)$$

As it is a marginal value, the output capacitance is set as $C_{out} = 0.200mF$.

To ensure that the simulation works properly, the time constant set by the capacitance and the load must be, at least, 10 times greater than the sampling time of the simulation.

$$\zeta = R_{load} \cdot C_{out} = 0.004s \gg 1 \cdot 10^{-6} \quad (eq. 12)$$

The input capacitance is set to be $C_{in} = 0.200mF$ and like the output capacitor it has been observed to be a value which minimizes the initial transient response of the current and voltage when simulating the system.

In case of having a desired output voltage of 72V, like the one of batteries commonly used in vehicles like scooters, the dimensions of the elements of the converter should be recalculated using the previously stated equations.

5.4.2 ALGORITHM FOR TRACKING THE OUTPUT VOLTAGE

The code used to define the duty cycle that should be inserted in the PWM Generator has been developed and can be found in *APPENDIX 3*. This algorithm tracks the output voltage of the converter and sets the adequate value of D necessary to reach the desired output voltage, in this case, 24V.

The starting value of the D is set to 0.8 and it is lowered or increased with $\Delta D = 0.01$ until the output voltage associated to it is 24V. In case the voltage of panels is not enough to reach 24V at the output, the established D is the corresponding to the maximum voltage that the panels are able to provide.

5.5 LOAD REGULATOR WITH MPPT ALGORITHMS

Finally, the converter previously designed is connected to a PV-array capable of simulating PSC and to a load consisting of a battery and a resistor to simulate the conditions that would occur in a vehicle. To study its behaviour, it will be implemented with both a Perturbation and Observation MPPT algorithm and with a Duty Sweeping algorithm similar to the one proposed in [3], (capable of working under PSC).

5.5.1 MODEL OF THE PHOVOVOLTAIC ARRAY

The simulation of partially shaded conditions implies the representation in *Simulink* of a photovoltaic array in which each panel can receive a different irradiance. Each panel represents one of the PV-panels from the Mechanical Engineering department.

The model is formed by three panels connected in series and each having a bypass diode connected in parallel. The function of these diodes is to protect the remaining panels in case the panel they are connected in parallel with, suffers a shading. When the panel is partially shaded, part of the current (or all the current in the case of a total shading) transits through the diode, avoiding the shaded panel and allowing the system to continue working [4].

By selecting the value of irradiance received by each panel, the partially shaded conditions can be represented and are ready to be used in the simulation. Next figure shows, as an example, the curves when one panel receives 1000W/m^2 , another panel receives 500W/m^2 and the last one receives 100W/m^2 :

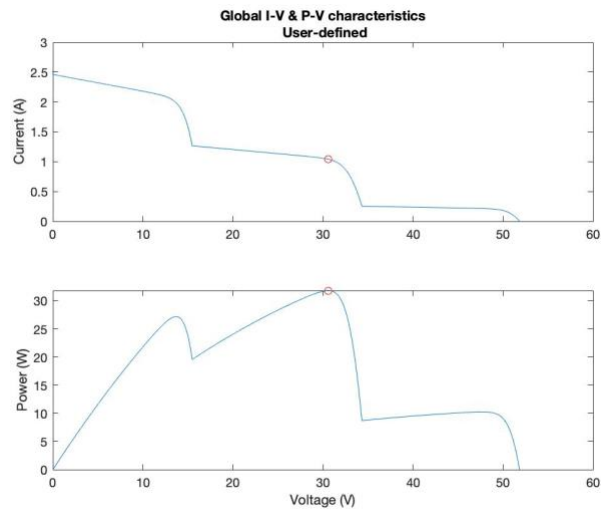


Figure 5.4: I-V and P-V curve of the array under PSC and 25°C

5.5.2 MODEL OF THE COMPLETE SYSTEM

The system modelled in *Simulink* counts with three differentiated areas. First, the model of the photovoltaic array, second the Boost converter acting as load regulator in-between the PV-array and the load, and finally the part of the load.

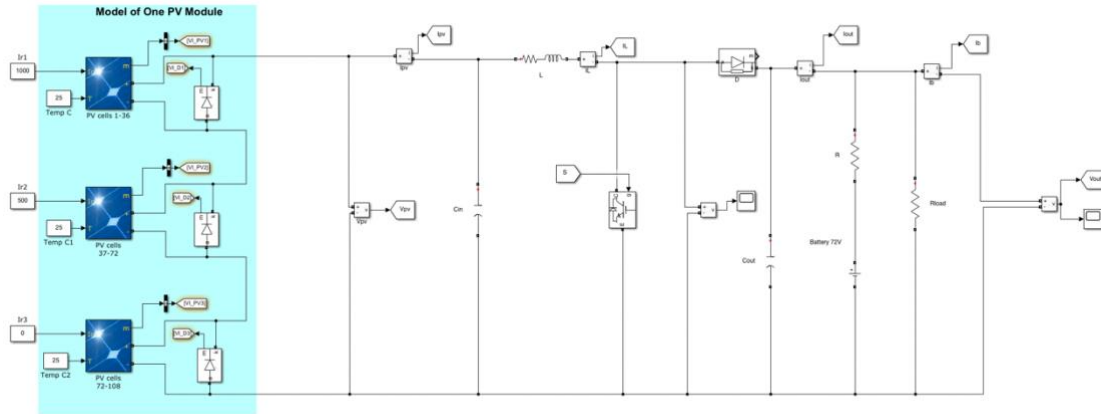


Figure 5.5: model of the system used in Simulink

The model of the PV-array has been explained above and the irradiance received by each panel can be modified at user's will.

The regulator consists of the Boost converter that has been shown in previous sections with some modifications in the values of its components as the load connected to its output varies. It has been seen that depending on the values the passive elements take; the operation of the system gets compromised and does not provide the expected response. The value of the inductor has been modified to $L=1\text{mH}$ to ensure that the power from the PV-array is transferred to the load and it is not transferred to ground and the capacitor at the input and output of the capacitor have set to $C_{in}=900\mu\text{F}$ and $C_{out}=200\mu\text{F}$ respectively. The frequency at the PWM generator is set to 10KHz as in the previous converter.

The load part of the model consists of a resistive load of 50Ω (it could be varied) which represents a load from the vehicle and a battery of 72V connected in series to small resistor (0.1Ω) which will be in charge of feeding the load when the irradiance is very low, and the PV-array is not able of giving it the required power and will also be charged with the power provided by the panels.

5.5.3 PERTURBATION AND OBSERVATION ALGORITHM

After having analyzed different techniques to carry out the MPPT in *section 4.2.2*, it has been decided that the most appropriate one for conducting a simulation and comparing it to Duty Sweeping is the Observation & Perturbation technique because it is a commonly used technique, it is quite simple and does not require the usage of logic control.

P&O is implemented in the controller of the regulator. The code implemented in MATLAB can be found in *APPENDIX 4*.

As stated in *section 4.2.2*, with this MPPT method small perturbations are applied to the voltage until the maximum power point is reached.

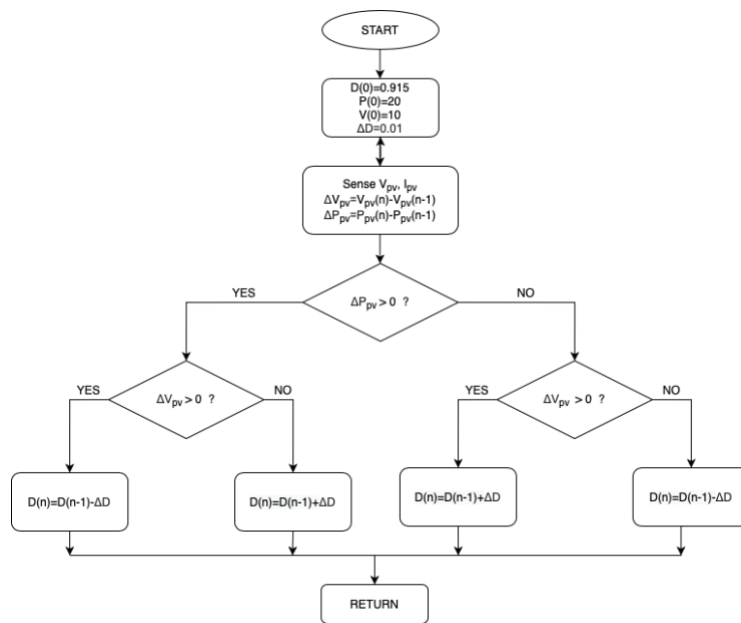


Figure 5.6: Perturbation & Observation method

5.5.4 DUTY SWEEPING ALGORITHM

A RMPPT method very similar to the one proposed in [3], is designed and implemented in MATLAB/Simulink can be found in *APPENDIX 5*).

This code works in the following way:

- 1) The algorithm is started.
- 2) The default parameters are defined. In this case, the sweeping of the duty cycle starts at $D=0.915$, considering power as zero and the duty cycle is swept in intervals of 0.01 .
- 3) For each duty cycle implemented, current and voltage are sensed, and the corresponding output power is calculated and stored.
- 4) Once all the duty cycles from 0.915 until 0.415 are applied (a total amount of 50 was defined), a comparison of all powers recorded, determination of the greatest one and determination of its corresponding duty cycle are carried out.
- 5) The duty cycle and output power determined in previous step are used as first references to carry out P&O.
- 6) P&O is carried out around the MPP until the output power decreases under 10% with respect to the previous output power. When this occurs, the system interprets that the irradiance has suffered a variation and returns to 3), where the DS procedure starts again.

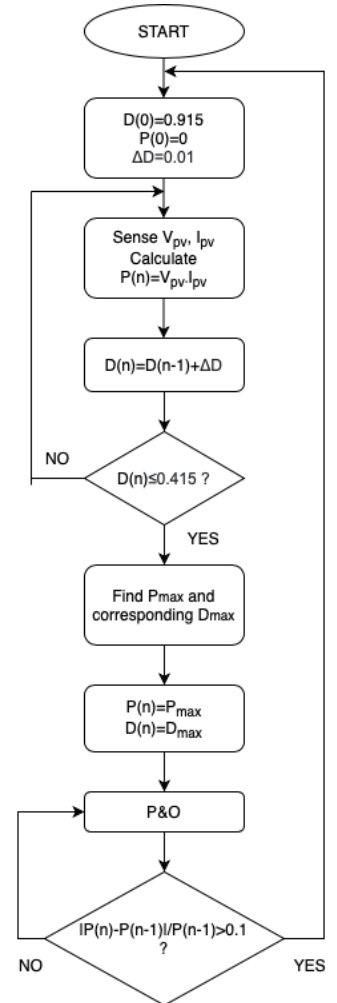


Figure 5.7: Duty Sweeping method

6. RESULTS

In this section, the results obtained after analyzing the data extracted in the experimental procedure for characterizing the panels and analyzing the simulations are shown.

Firstly, the characteristic curves of the photovoltaic panels provided by the Mechanical Engineering department are presented so that their characteristic parameters can be later used in the characterization of the photovoltaic panels used in the simulations of the photovoltaic systems.

Secondly, the operation of the commercial load regulator is verified to understand how does a regulator work.

Thirdly, the results after simulating a Boost converter feeding a load with constant voltage are presented. This converter is not controlled by a MPPT algorithm, but it serves as an initial contact with the program MATLAB/Simulink in order to study the critical parameters of the converter (values of L , C_{in} and C_{out}) and the simulation (sampling frequency, switching frequency of the PWM generator, variation of the duty cycle).

Finally, a Boost converter is simulated with 2 algorithms that track the MPPT and their behavior under PSC are compared.

6.1 CHARACTERISTIC CURVES OF THE PANELS

By analyzing and arranging the data exposed in *APPENDIX 1*, the following characteristic curves, at a mean ambient temperature of 18°C can be extracted. Due to the variable weather conditions, the irradiances recorded were constantly varying. That is why all the data has been divided in blocks and each one has been assigned the mean irradiance value.

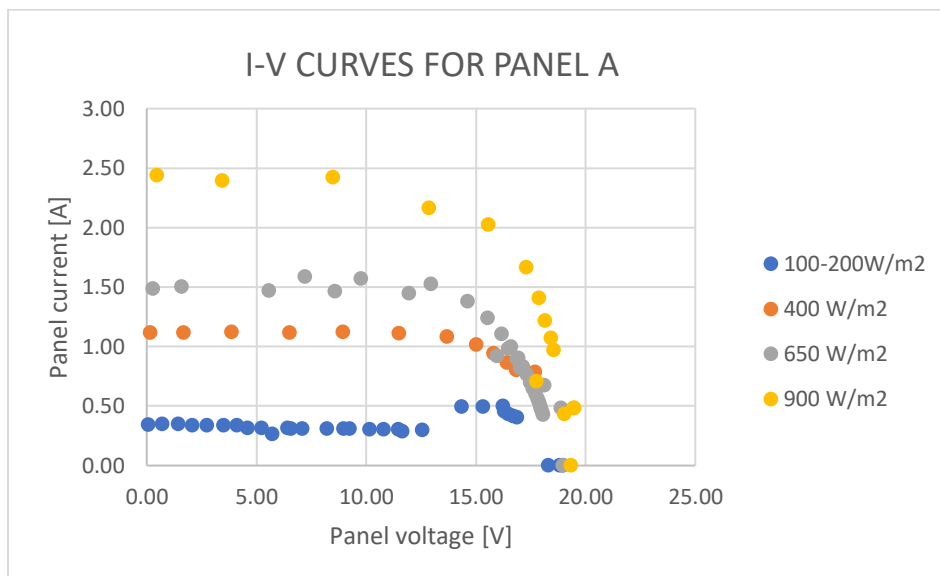


Figure 6.1: I-V curve for panel A at 18°C

The curves obtained for panel A respond to the expected model. The higher the irradiance the higher the short-circuit current and, as the temperature is maintained constant, the open circuit voltage is common for all irradiances.

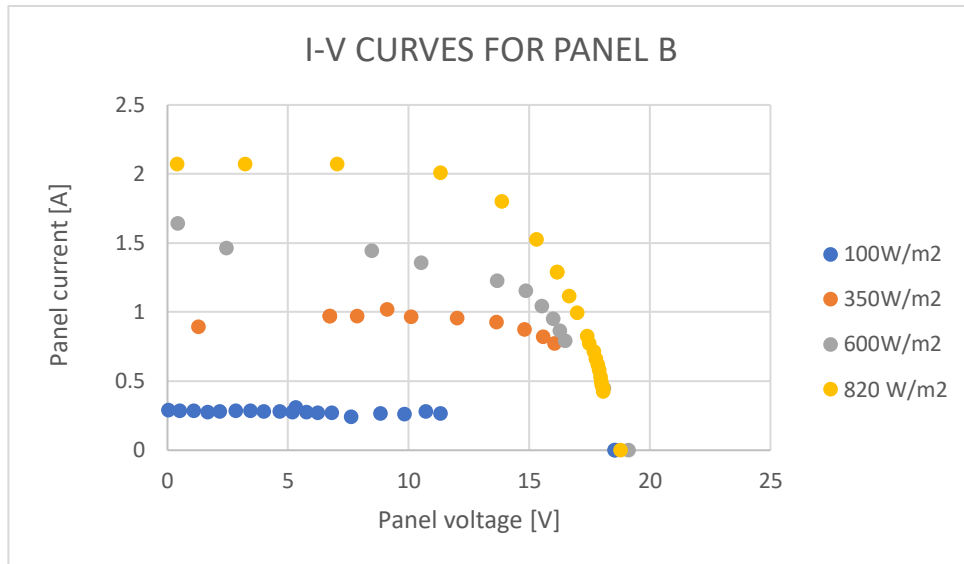


Figure 6.2: I-V curve for panel B at 18°C

For panel B, some discontinuities are found. They are due to the variability of the irradiance and the impossibility to record the values of current and voltage for each position of the resistors and for each value of the irradiance.

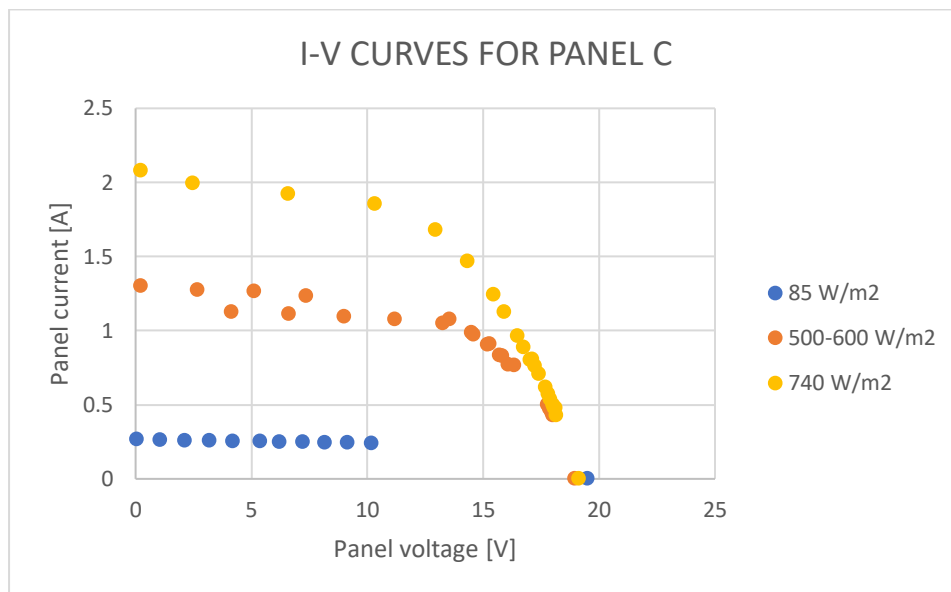


Figure 6.3: I-V curve for panel C at 18°C

The characteristic curve for panel C being reached with an irradiance of about 300-400 W/m² has been impossible to draw. However, for the other values of irradiance, the curves have an acceptable continuity.

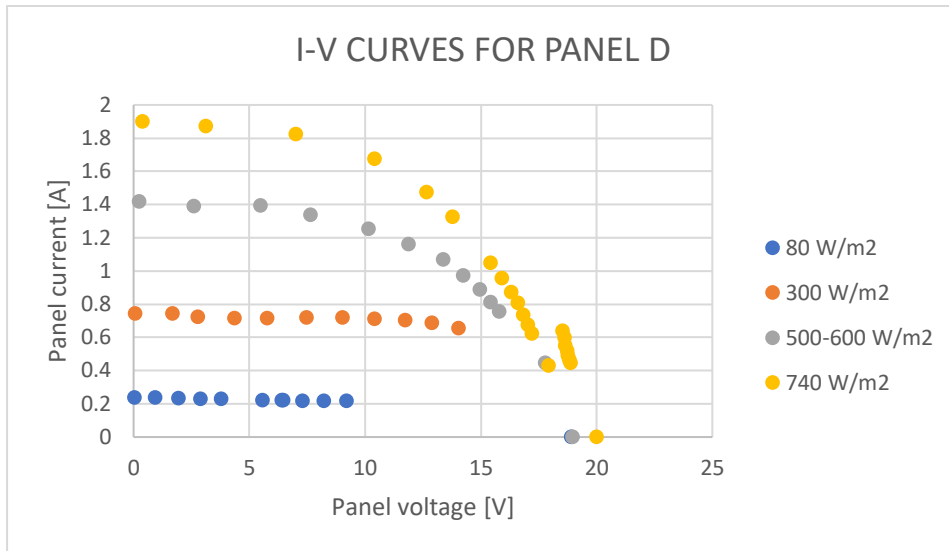


Figure 6.4: I-V curve for panel D at 18°C

In addition, for low values of irradiance (specially for panels C and D), the currents near the open circuit voltage, are difficult to measure as great values of resistance are needed to reach those values of current.

6.1.1 POWER-VOLTAGE CURVES OF THE PANELS

The power extracted from the PV-panels can be estimated from the previous characteristic I-V curves:

$$P = V \cdot I \quad (\text{eq. 13})$$

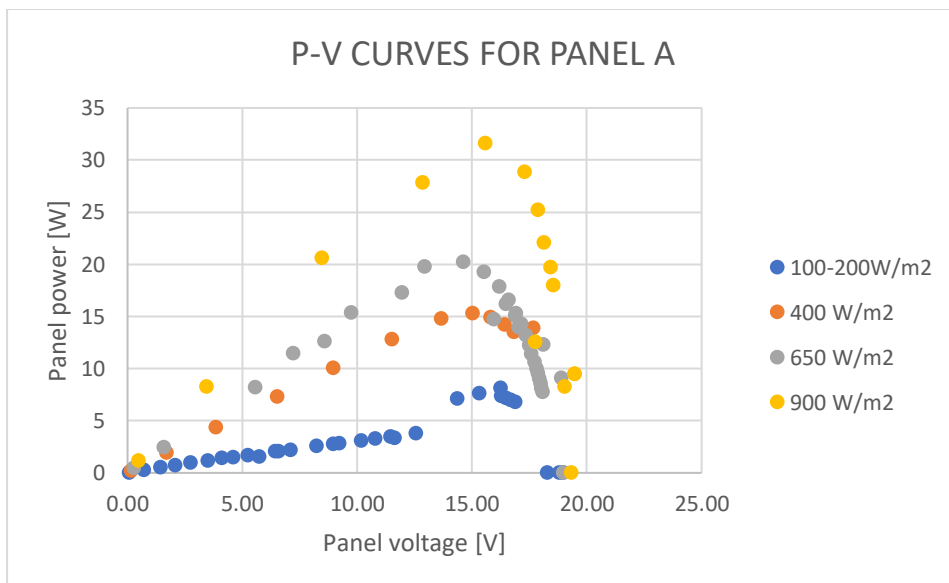


Figure 6.5: P-V curves for panel A

As for the I-V curves, they are as expected. The MPP at every irradiance coincides with the same voltage (15V).

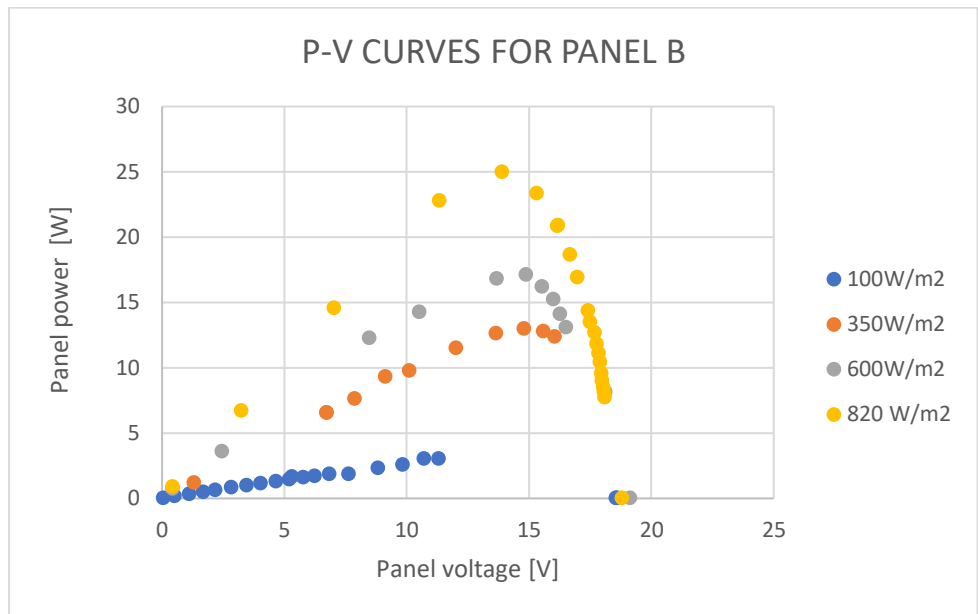


Figure 6.6: P-V curves for panel B

In panel B, the MPP is also located at $V=15V$. For the irradiance of $100W/m^2$, there is a lack of information about the MPP but it can be estimated to be at 15V too.

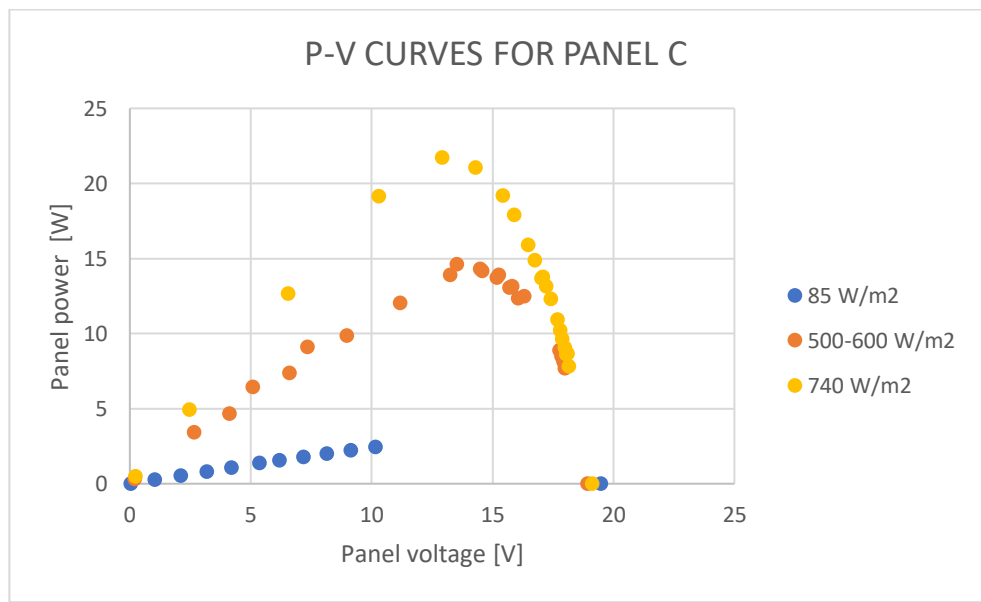


Figure 6.7: P-V curves for panel C

Panel C shows its MPP at a voltage a bit lower (13V) for the irradiances of 740 and 500-600W/m² and there is also some information missing on the 85W/m² curve.

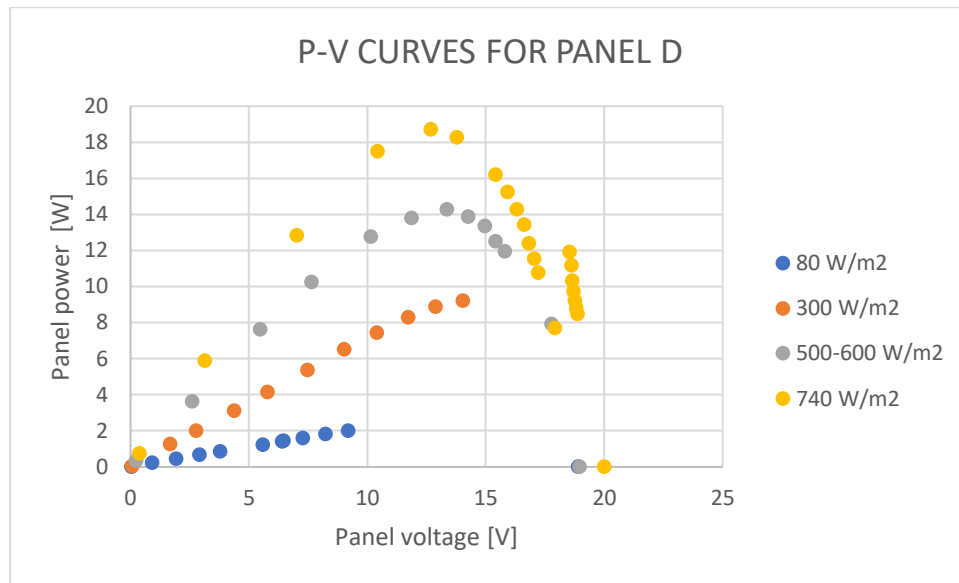


Figure 6.8: P-V curves for panel D

Panel D also shows clearly its MPP at 13V for 740W/m² and 500-600W/m². For 300 and 80W/m² there is some information missing to complete the curve but, for 300W/m², the MPP seems to be located at a bit higher voltage, at 14V.

With the previous power curves, the maximum power point for each PV panel in terms of current (I) and voltage (V) is deduced. This value is important as it marks the maximum output power that can be extracted from the PV panels. The maximum power obtained for each of the panels and the voltage at which it is reached are presented in the next table:

Table 6.1: Maximum power extracted

| PANEL | IRRADIANCE (W/m ²) | MAXIMUM POWER (W) | VOLTAGE AT MAX. POWER (V) |
|---------|-----------------------------------|----------------------|------------------------------|
| PANEL A | 900 | 31.58 | 15 |
| PANEL B | 820 | 24.99 | 15 |
| PANEL C | 740 | 21.71 | 13 |
| PANEL D | 740 | 18.69 | 13 |

As the measurements are carried out under random ambient conditions, the maximum values of irradiance that have been achieved vary from one panel to another and are different to the standard conditions considered in laboratories where the specifications for P-V panels are measured. If these measurements are carried on other location or in a different moment of the year, greater values of maximum power would be recorded.

It would seem, though, that the behavior of the panels is quite similar. For an irradiance of 900 W/m^2 (maximum achieved on panel A), the estimated power for panels B, C and D would be similar to the power obtained in A.

For the objective of simulating the load regulator in MATLAB/Simulink, the previous I-V and P-V curves are essential as their information will be introduced in the blocks corresponding to the panels. The parameters introduced in the block are:

$$V_{oc}=18\text{V}, \quad I_{sc}=2.5\text{A}, \quad P_{max}=30\text{W}, \quad V_{mpp}=15\text{V} \quad \text{and} \quad I_{mpp}=2\text{A}.$$

Due to some limitations of MATLAB/Simulink, the difference between V_{mpp} and V_{oc} must be lower than 3V. Consequently, they differ a bit with respect to the real values as the real V_{oc} was 20V.

6.1.2 BEHAVIOUR OF THE P-V PANELS UNDER PARTIALLY SHADED CONDITIONS

Once the characteristic curves of the panels under constant conditions have been characterized, it is important to know how they behave under partially shaded conditions. During the experimental procedure, the irradiance received by panel D was around 750W/m^2 and the irradiance of panel A was 0 W/m^2 as the panel was covered.

The expected curves of the array -obtained with a Simulink model designed with the information of previous section- formed by panels A and D under PSC are similar to the following ones:

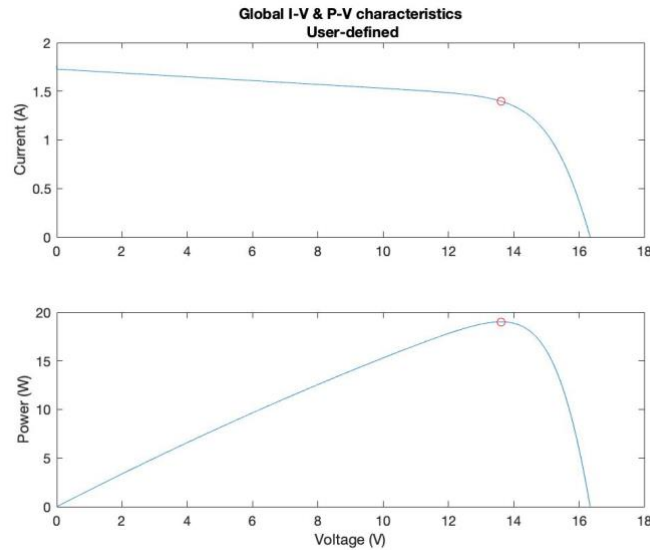


Figure 6.9: Theoretical I-V and P-V curves under PSC obtained in MATLAB/Simulink

As panel A is completely shaded, it has no contribution to the power and current generated by the array and the curve expected is like the curve of a single panel under constant irradiance of 750W/m^2 .

Whereas the curves obtained experimentally are the following ones:

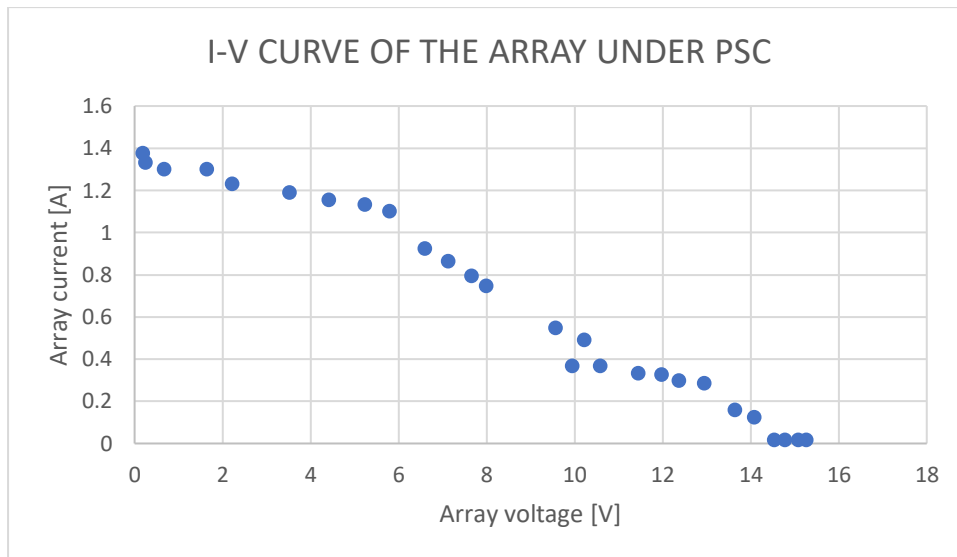


Figure 6.10: I-V curve obtained experimentally under PSC

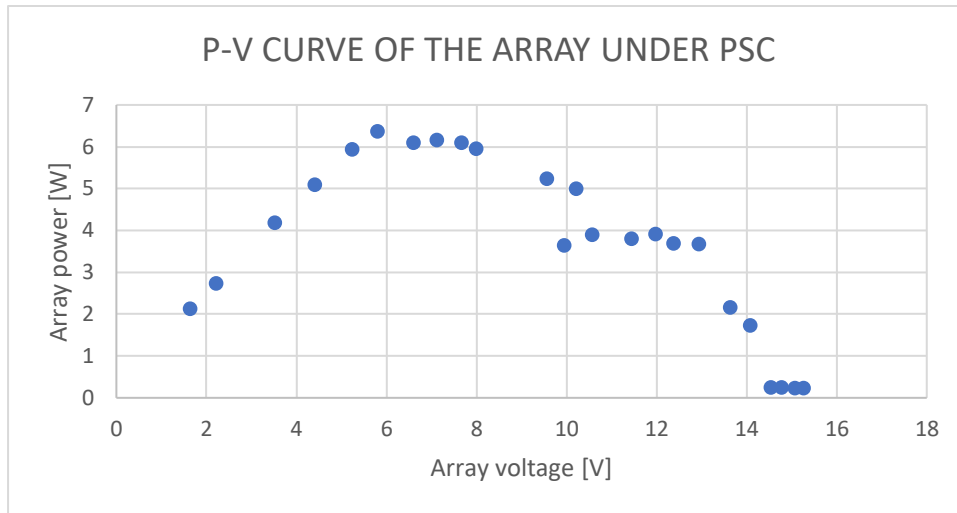


Figure 6.11: P-V curve obtained experimentally under PSC

In general aspects, the theoretical and the calculated curves have a similar shape. Several differences can be observed between the expected and the real curves. First, the short-circuit current is smaller in the real curves (it is 1.4 A whereas the expected value was 1.7A). The open-circuit voltage, however, is quite similar to the expected one. Regarding the power, the maximum power recorded is around 38% of the maximum power expected and it takes place when voltage is 6V instead of 13V.

The disparity between the curves may arise due to the imprecision at the measurements, due to the connection between the panels (which could produce losses) or due to the variability of the irradiance.

6.1.3 EFFECT OF AMBIENT TEMPERATURE ON THE CHARACTERISTIC CURVE

After having characterized the I-V curves for the 4 photovoltaic panels, the characterization of one of them (panel A) is repeated 2 months later to study if a higher ambient temperature has any impact on the behavior of the panels.

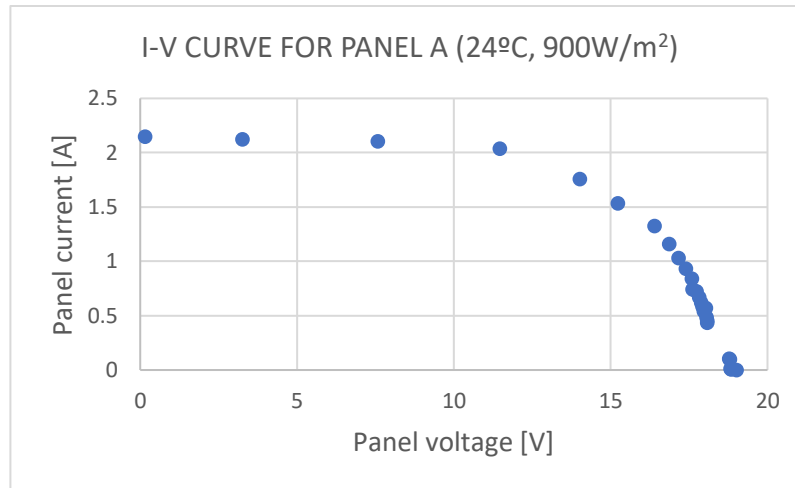


Figure 6.12: I-V curve for panel A at 24°C

The results of this characterization are found in *APPENDIX 6*.

The average ambient temperature when characterizing the curves for the first time was 18°C whereas on the second trial it is 24°C. The irradiance found in the second trial was 900W/m², consequently these results can be compared to the ones of *figure 6.1* for an irradiance of 900W/m².

For an increase in temperature of 33%, short circuit current decreases an 11.89% whereas open circuit voltage decreases 1.55%.

* *APPENDIX 7* includes some verifications and relations that have been deduced when studying the behaviour of the four panels from the Mechanical Engineering department. They are not significant for the scope of this project; however, they could be interesting for future research about these panels.

6.2 VERIFICATION OF THE OPERATION OF THE COMMERCIAL LOAD REGULATOR

To verify if the regulator operates properly in the different conditions, the measured values are going to be compared to the ones extracted from the characteristic curves which are the ones that should be theoretically obtained.

For configuration 1, with the four panels facing the Sun, the extracted power should be around 104W as the maximum power from the PV panels is approximately 35W for panel A, 25W for B and 22W for panel C and panel D each.

The measured voltage and current at the input of the regulator are $V_{\text{PANELS}} = 26.43\text{V}$ and $I_{\text{PANELS}} = 4.112\text{A}$ so the power supplied is 108.7W.

For configuration 2, the behavior is similar: from the first string (A and B), the expected power is around 8W from each panel as they are shaded and from the second string, the expected power is the same as previous, around 41W. The total expected power is around 57W and the power obtained is 60W as $V_{\text{PANELS}} = 25.16\text{V}$ and $I_{\text{PANELS}}=2.401\text{A}$. The problem in this case is that the power extracted from the PV array is not sufficient to feed the load, thus, the batteries contribute to feed the lamp.

For configuration 3, the expected power is around 60W (25W from B and 19W from D which are not covered and 8W from both A and C which are shaded). Nevertheless, the measured value for power is 17.03W as $V_{\text{PANELS}} = 24.47\text{V}$ and $I_{\text{PANELS}}=0.696\text{A}$. This reflects that the regulator is not carrying out the MPPT correctly as it is not extracting the maximum power available. As the load regulator does not work properly in this case, the batteries contribute to the input of current to the luminous load.

The expected power for configuration 4 is approximately 55W and the real power extracted from the panels is 55.6W. Although the regulator extracts the maximum power available at its input, the load requires more power, so the batteries feed it.

For configurations 1, 2 and 4 where at least one string is completely facing the Sun, the behavior of the load regulator is correct as it extracts the maximum power available from the panels. However, for configurations 2 and 4, the extracted power from the panels is not sufficient to feed the load and the batteries give power to the load. As a consequence, the batteries are discharged.

For configuration 3, where the photovoltaic setup is partially shaded, the load regulator is not capable of extracting the maximum power from the panels. Under these conditions, the power curve of the array presents different maxima (2 in this case). In

these cases, when the load regulator reaches a maximum of the curve, it keeps oscillating around it and sets it as operation point (MPP according to the control algorithm of the regulator), but it does not differentiate between the absolute maximum of the curve (corresponding to the MPP) and any of the local maxima, consequently, the operation point is not the one corresponding to the maximum power extraction.

In order to ensure the extraction of the maximum power of the photovoltaic array, the load regulator must include a different MPPT algorithm, one capable of working under PSC.

6.3 SIMULATION OF THE BOOST CONVERTER FEEDING A LOAD WITH CONSTANT VOLTAGE WHILE TRACKING THE OUTPUT VOLTAGE

The diagram of the Boost converter providing a constant output voltage is simulated in MATLAB/Simulink, for the parameters used to design it, a single panel receiving an irradiance of 1000W/m^2 , with a switching frequency of 10KHz

The results of the simulation are the following ones:

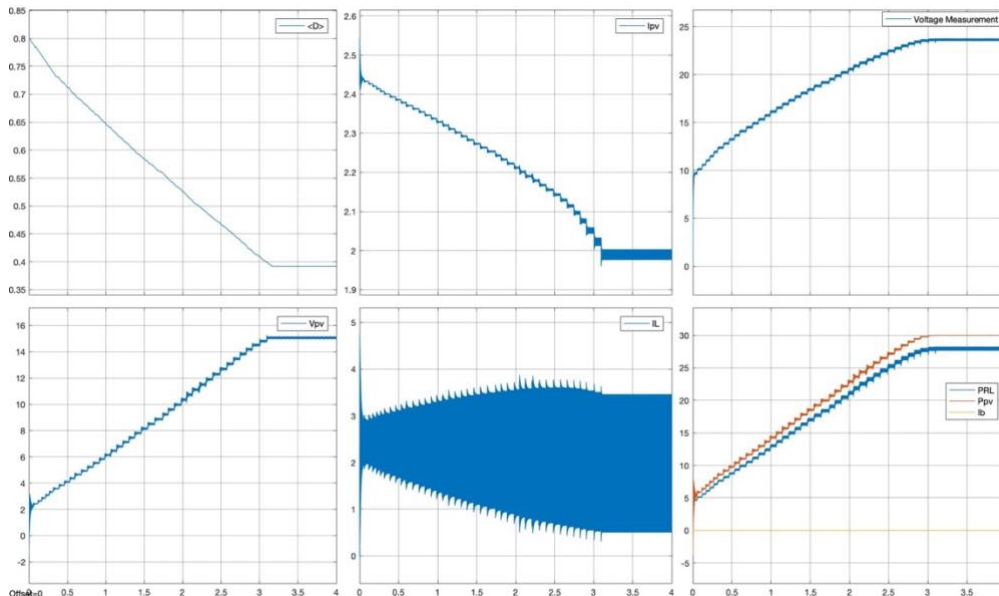


Figure 6.13: Simulation with one panel feeding the load with an irradiance of 1000W/m^2

It is observed that the voltage at the load (*Voltage measurement*) does not reach the expected value, 24V (it only reaches 23.6V) and the duty cycle is not the estimated one too, it is 0.41 instead of 0.375. The reason why this happens is because initially, the power transfer from the panel to the load has been assumed with no losses but, part of the power at the input is consumed by the semiconductors. Thus, it is impossible to transfer the 28.8W to the load (which is the power that makes it have 24V on its terminals) as more than 1.2W are lost from the 30W provided by the panel. In this case the regulator achieves a power efficiency of:

$$\eta = \frac{P_{out}}{P_{pv}} \cdot 100 \approx \frac{28.8}{30} \cdot 100 = 96\% \quad (eq. 14)$$

Next, the diagram is simulated with an array of two panels in series and now, the power in the input is enough to reach the voltage setpoint at the output.

The 24V and 28.8W at the output are achieved as the power and voltage that can be provided by the input is double than the one in the previous case. In this respect, the duty cycle is $D=0.48$ with $I_{pv}=2.34A$ and $V_{pv}=13V$, far away from the maximum power point as now, the maximum power that can be provided by the array is 60W and only 31W in the input are necessary to fulfill the requirements of a constant value at the output. In this case, the efficiency is 94.67%.

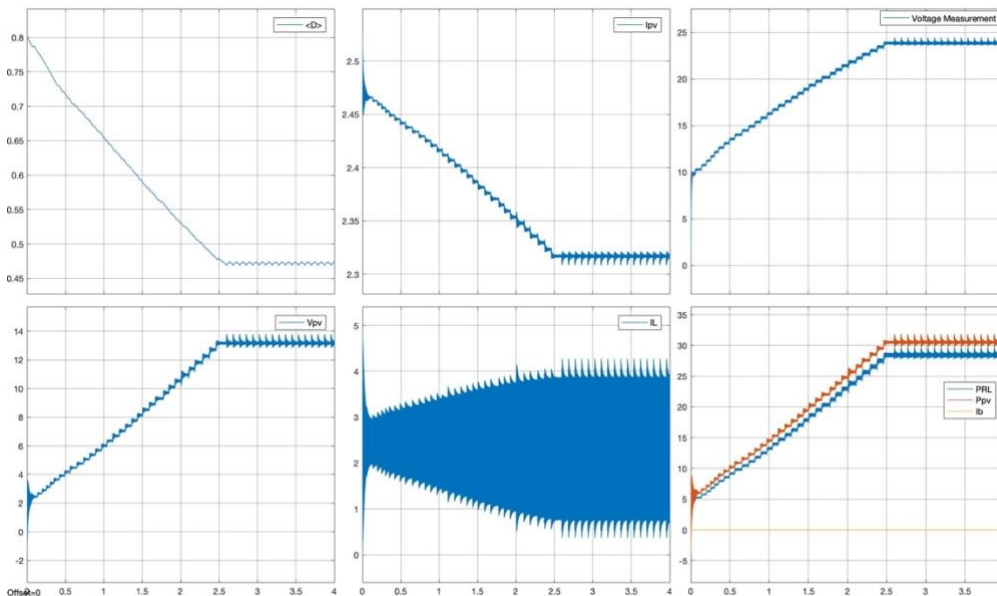


Figure 6.14: Simulation with 2 panels in series feeding the load with an irradiance of 1000W/m²

As it has been stated in *section 5.4.1* the load connected to this converter could have a value of 20 Ω or higher. Next figure reproduces the situation above (1 string of 2

panels and $1000\text{W}/\text{m}^2$) but with a resistance of $40\ \Omega$ to show that the algorithm works for higher values of resistance, too.

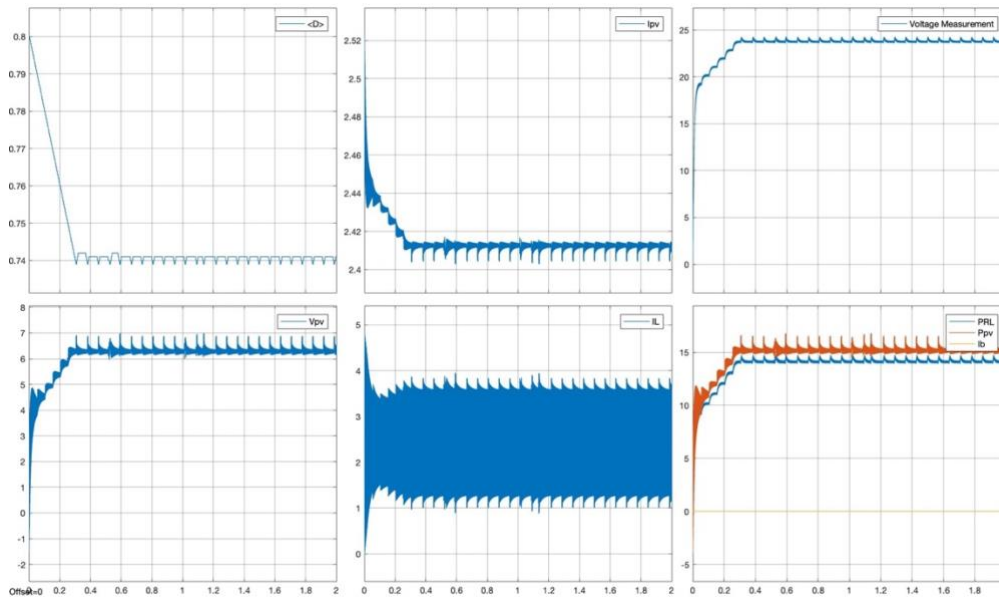


Figure 6.15: Verification for a load of $40\ \Omega$

Thus, as the resistance is double, the voltage from the panels and the power transmitted to the load is half but the voltage at the load is maintained as desired, at a constant value of 24V . The value of D in this case varies as the operation point is no longer the one of maximum power which is the corresponding to a load of $20\ \Omega$ (see section 5.4.1).

Subsequently, several simulations are carried out to see which the requirements of the PV-array are to get a constant output of 24V at the output of the converter and the results are the following ones:

- If irradiance is equal to $1000\text{W}/\text{m}^2$, a minimum of two panels (from the ones available in the laboratory) in series are required.
- If irradiance is lower, and equal to $500\text{W}/\text{m}^2$, then a minimum of 2 strings (consisting of 2 panels in series each) in parallel are necessary.
- If irradiance is reduced to $100\text{W}/\text{m}^2$, 7 strings (of 2 panels in series each) connected in parallel are the minimum required to supply the setpoint of 24V at the output of the system.

For all these simulations, the current passing through the inductor (I_L) has been carefully checked to be greater than 0. The value of the inductor was calculated in order to avoid the current through it to be negative. Because if I_L decrements below 0, discontinuous conduction mode takes place. In this situation the inductor gets discharged at the end of the working cycle and the output voltage does not longer depend only on the D and the input voltage. It would also depend on other parameters like I_L and the switching frequency. As the algorithm used relies on the relation of V_{out} with V_{pv} and D , the converter could malfunction.

EFFECTS OF CRITICAL PARAMETERS OF THE CONTROLLER

The sampling frequency, the switching frequency of the PWM and the variation of D are parameters which determine how the microcontroller works and how is the response of the system.

VARIATION OF D

The previous converter is now fed by a panel receiving first, a certain value of irradiance and, after some seconds, another value of irradiance. To carry out this in *Simulink*, the irradiance input of the panel is connected to a pulse function which allows to sweep from one value of irradiance to another.

Each time the irradiance changes, the converter must change its duty cycle to adapt it to the new conditions. A determinant factor in response of the system is the duty cycle D , specifically, the amplitude of its variation. The greater the variation of the D in each iteration, the shorter that it will take to reach the correct D .

The next figures show the same simulation, with an initial irradiance of 1000W/m^2 , changing 2 seconds later to an irradiance of 500W/m^2 and 2 seconds later returning to 1000W/m^2 . The first one is carried out with a variation of D , $\Delta D = 0.01$ and the second one with $\Delta D = 0.1$.

For these simulations, the configuration of the P-V array considered is the one of 2 strings in parallel having each string 2 panels in series and the value of D varies from 0.75 with 1000W/m^2 to 0.48 with 500W/m^2 .

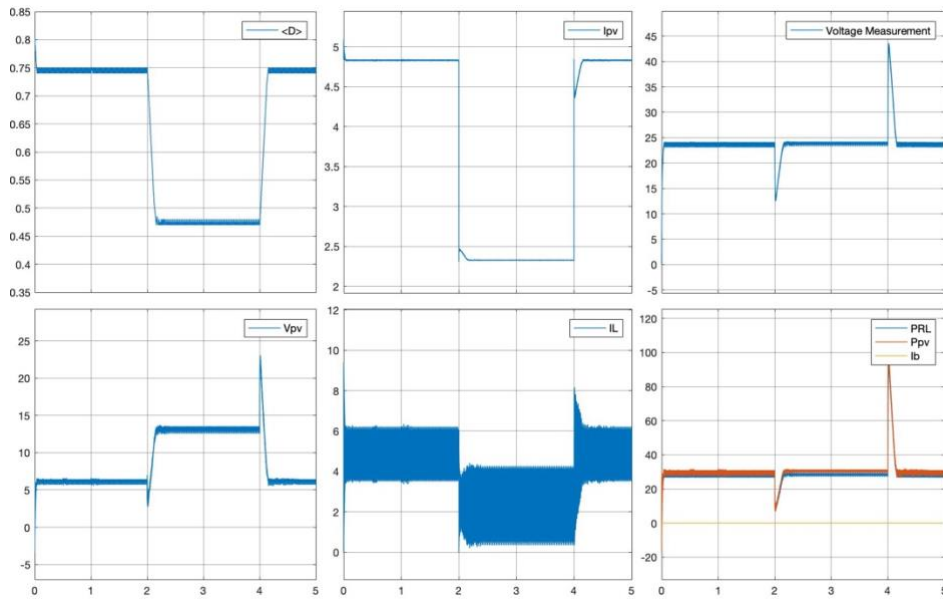


Figure 6.16: Simulation with 2 strings of 2 panels in series with a variable irradiance and $\Delta D=0.01$

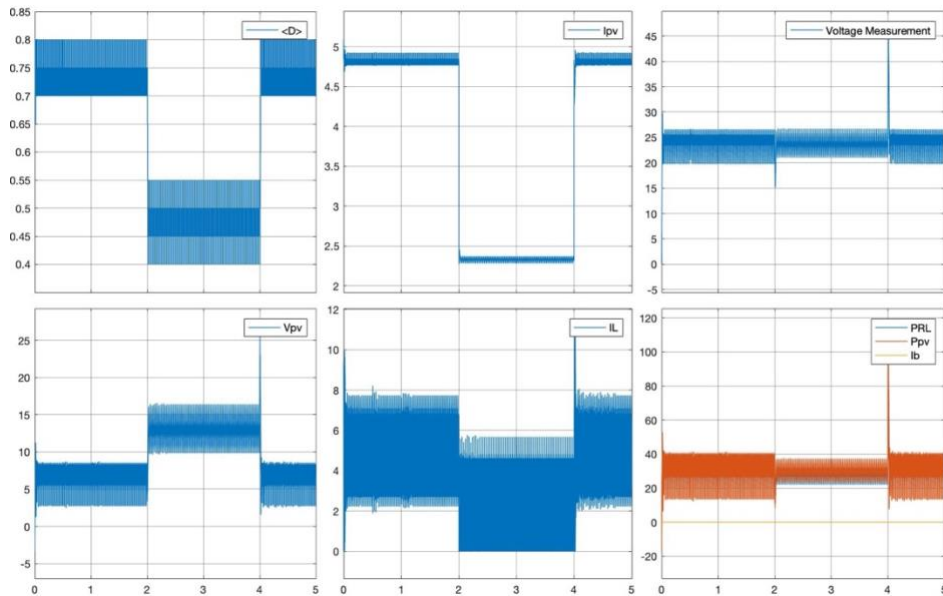


Figure 6.17: Simulation with 2 strings of 2 panels in series with a variable irradiance and $\Delta D=0.1$

In the first case, with a lower value of ΔD , the system takes a longer time to reestablish the setpoint of the output voltage when the irradiance value decreases. In the second case, with a greater D , the system almost instantaneously varies the operation point to the setpoint.

Nevertheless, drawbacks are observed when ΔD is set to 0.1. The response is much more unstable, the ripple at the output signals is increased as the variation of the input signals are also more abrupt, and the discontinuous conduction mode is reached.

SWITCHING AND SAMPLING FREQUENCIES OF THE CONTROLLER

The simulation of the converter being fed by two panels under an irradiance of $1000\text{W}/\text{m}^2$ is now carried out for the next combination of switching frequencies and sampling frequencies:

Table 6.2: frequencies of the simulations

| | | | |
|---------------------------|-----|-----|-----|
| SWITCHING FREQUENCY (KHz) | 20 | 10 | 1 |
| SAMPLING FREQUENCY (Hz) | 100 | 200 | 500 |

For a switching frequency of 1KHz and sampling frequencies of 100 and 200Hz, the system does not respond correctly. The D is reduced until 0.7 (it should be established at around 0.48), the voltage and the power at the panels take negative values, the output voltage is maintained constant at 5V, and DCM appears in the inductance.

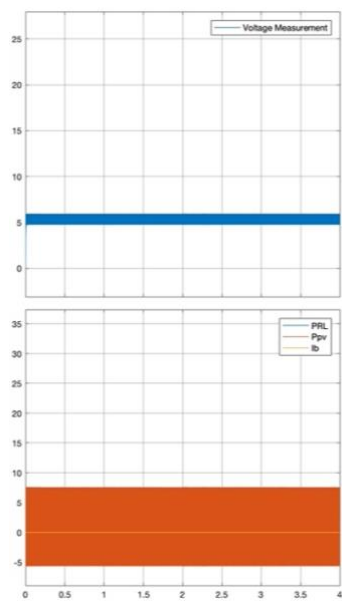


Figure 6.18: Simulation with 1KHz and 200Hz

With a switching and sampling frequencies of 1KHz and 500Hz respectively, the system can reach the voltage reference point of 24V. However, DCM can also be observed, the voltage and power variables also show negative values, and the ripple is unacceptable.

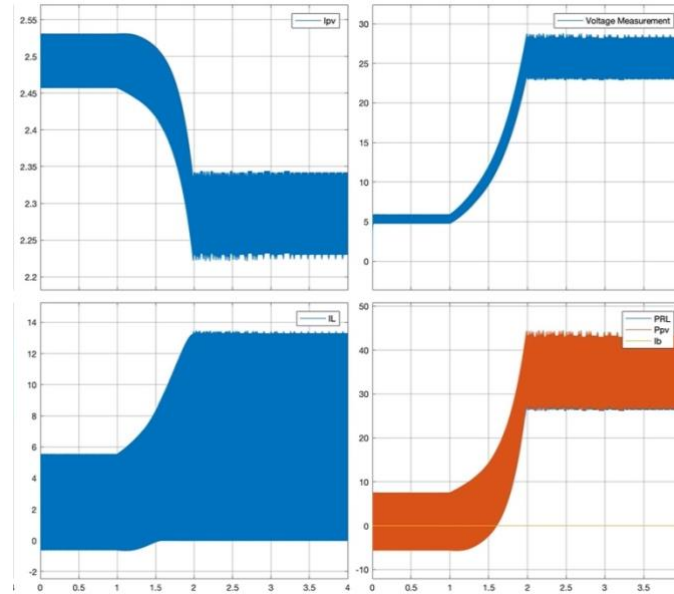


Figure 6.19: Simulation with 1KHz and 500Hz

All simulations with switching frequencies of 10 and 20KHz (except for the simulation with 20KHz and sampling frequency of 100Hz) converge to the setpoint output voltage (24V) and to a duty cycle of 0.48 (figure 6.14 shows the simulation with 10KHz and 200Hz). Nevertheless, some differences can be observed among them.

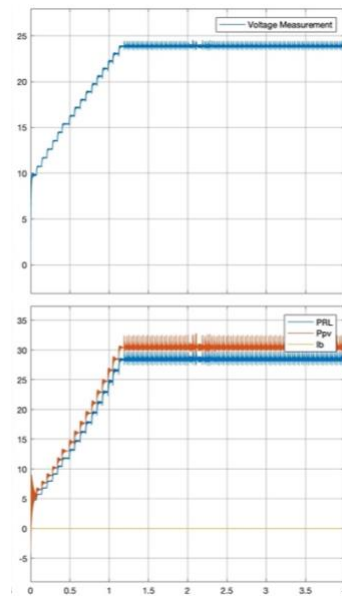


Figure 6.20: Simulation with 20KHz and 500Hz

The higher the sampling frequency, the quicker the 24V setpoint is reached (for 500Hz it takes around 1 second, for 200Hz around 2.5s and for 100Hz around 5s).

With switching frequency of 10KHz, the ripple at the measured variables is lower. This result could be expected as it is the frequency for which the converter has been designed.

The simulation with switching frequency of 20KHz and sampling frequency of 100Hz does not reach the setpoint, it can only reach 21V ($D=0.54$ instead of 0.48). Even though the response of the system is incorrect in this case, the oscillations of the variables are almost imperceptible:

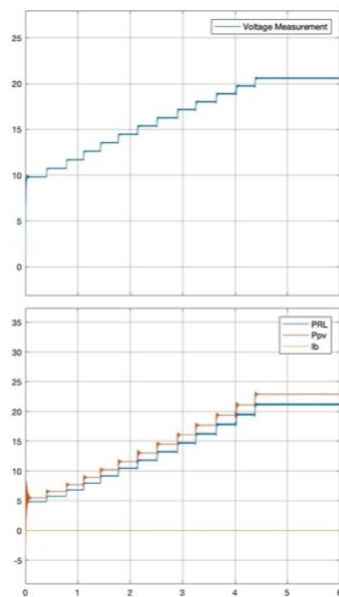


Figure 6.21: Simulation with 20KHz and 100Hz

As a result from previous simulations, it may be stated that, an equilibrium must be reached when deciding the value of ΔD . It must be sufficiently high so that the system is not too slow, but it will be limited by the maximum ripple permitted at the output. Regarding the switching frequency and sampling frequency of the controller, it has been shown that they must be carefully chosen as they determine the response of the system. The converter works well for high switching frequencies (10-20KHz) and sampling frequencies around 200-500Hz.

6.4 SIMULATION OF THE BOOST CONVERTER TO CARRY OUT MPPT UNDER PARTIALLY SHADED CONDITIONS

When trying to simulate the system both with the P&O algorithm and the Duty Sweeping algorithm, many difficulties have been encountered. The responses expected have not been reached until many modifications have been carried out in the Simulink model.

The values of the elements of the converter estimated in *section 5.4.1* had to be modified, the L had to be increased to 5mH to avoid discontinuous conductance mode in the inductor and the input capacitor had to be increased to 0.9mF to maintain the voltage of the panels.

Then, with 3 panels, the output voltage range is very big (almost 60V), consequently the required inductor is also big (5mH). As the L is so big, the system is slower, and it takes 250ms each time D is varied to get a stable response of the power (during this time voltage and current oscillate and the calculated power at the controller is not reliable). Hence, the sampling time must be set to 250ms, and the simulation is very slow.

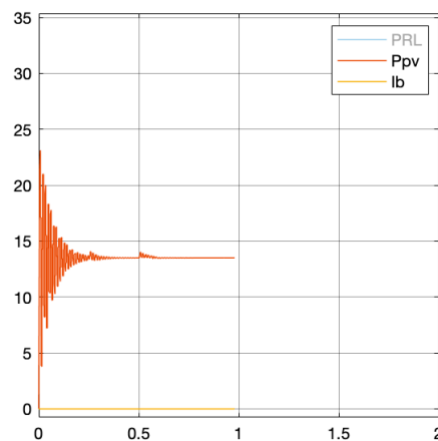


Figure 6.22: Time required for a stable response

To reduce the system's time constant to carry out the simulations in a shorter time, the irradiance of one of the panels is set to 0 permanently to simulate an array of only two panels in series. In this case, the voltage range is smaller (35V), so a smaller L is used (1mH) and the sampling time can be reduced to 50ms.

Moreover, the initial D in the simulations cannot be set to a value greater than 0.915 because the oscillations in the variables are also increased for bigger values of D.

6.4.1 SIMULATION WITH PERTURBATION AND OBSERVATION ALGORITHM

The characteristic curve for the array of two panels receiving one of them 1000W/m² and the other one 500W/m² is the following one:

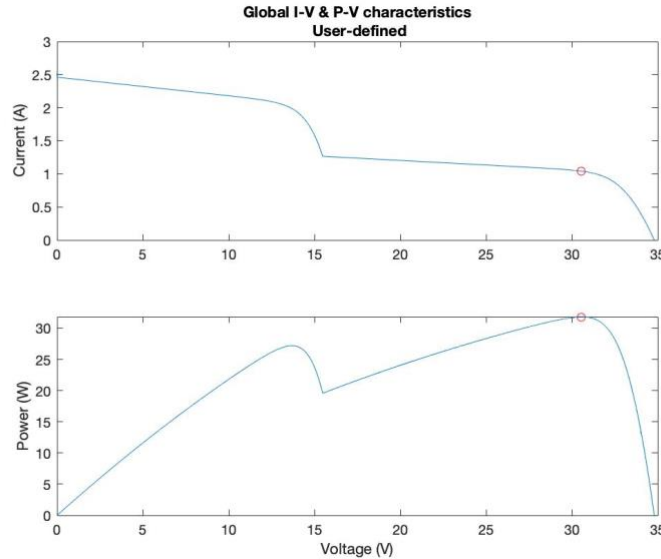


Figure 6.23: Characteristic curves of the simulated array under PSC

When the load regulator working with P&O is set under these conditions with an initial D of 0.915 and initial voltage and power of 10V and 20W respectively, the maximum power that the converter reaches is 27W (with D=0.8 and output voltage of the panels $V_{pv}=14V$), which is the power corresponding to the local maximum closer to the initial conditions but not the maximum power available (32W). The efficiency of the regulator is:

$$\eta = \frac{P_{out}}{V_{pv} \cdot I_{pv}} \cdot 100 \approx \frac{27}{14 \cdot 2} \cdot 100 = 96.45\% \quad (eq. 15)$$

STUDY ON PARTIALLY SHADED CONDITIONS REGULATORS FOR PV BASED ELECTRICALLY POWERED VEHICLES

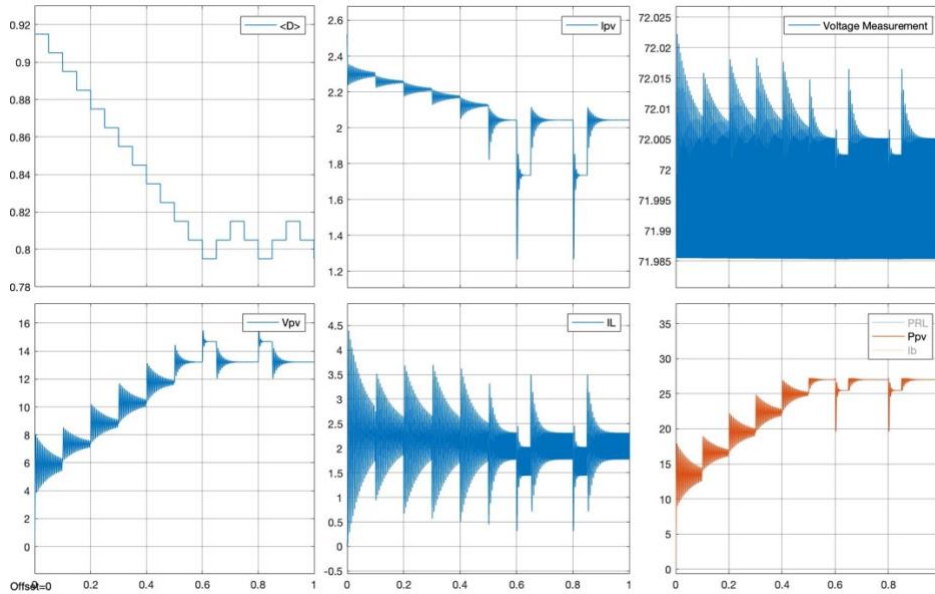


Figure 6.24: Simulation of P&O algorithm with initial $D=0.95$

Only if the initial D was set to a value corresponding to a closer value of the P-V panels absolute maximum power, the latter could be reached.

In the next figure the initial D is set to 0.5 and the initial voltage and power are set to 25V and 20W, reaching the absolute maximum ($D=0.57$, $V_{pv}=30V$, $P_{pv}=32W$):

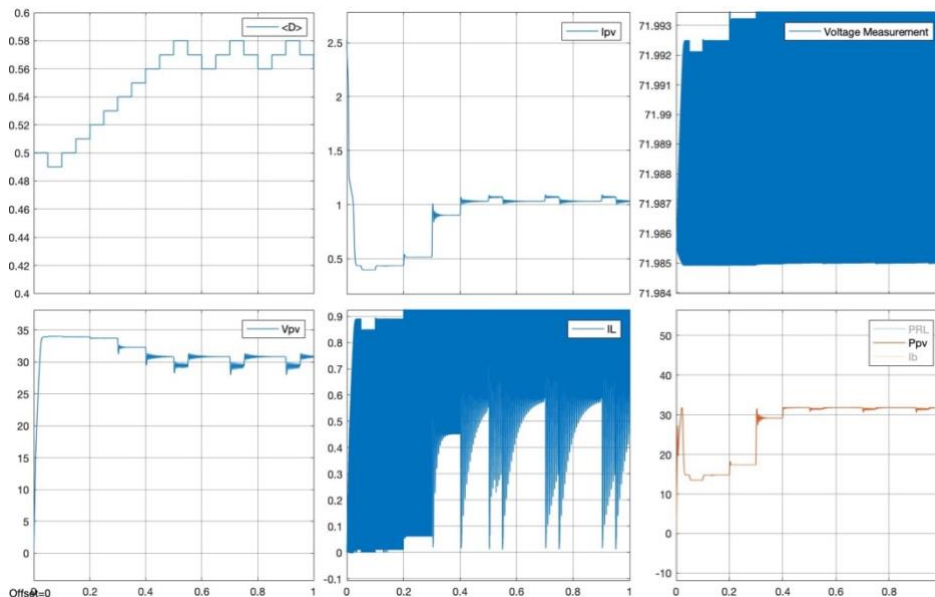


Figure 6.25: Simulation of P&O algorithm with initial $D=0.5$

In this case the efficiency of the regulator is:

$$\eta = \frac{P_{out}}{V_{pv} \cdot I_{pv}} \cdot 100 \approx \frac{32}{30 \cdot 1.1} \cdot 100 = 96.97\% \quad (eq. 16)$$

However, when irradiance conditions change, or more panels are set in the array, the maximum power point will move in the curve and another local maximum will be found instead of the absolute maximum. Consequently, P&O method is not convenient when PSC are expected.

6.4.2 SIMULATION WITH DUTY SWEEPING ALGORITHM

The Duty Sweeping algorithm is implemented in the load regulator and simulated for the same irradiance conditions as the P&O algorithm:

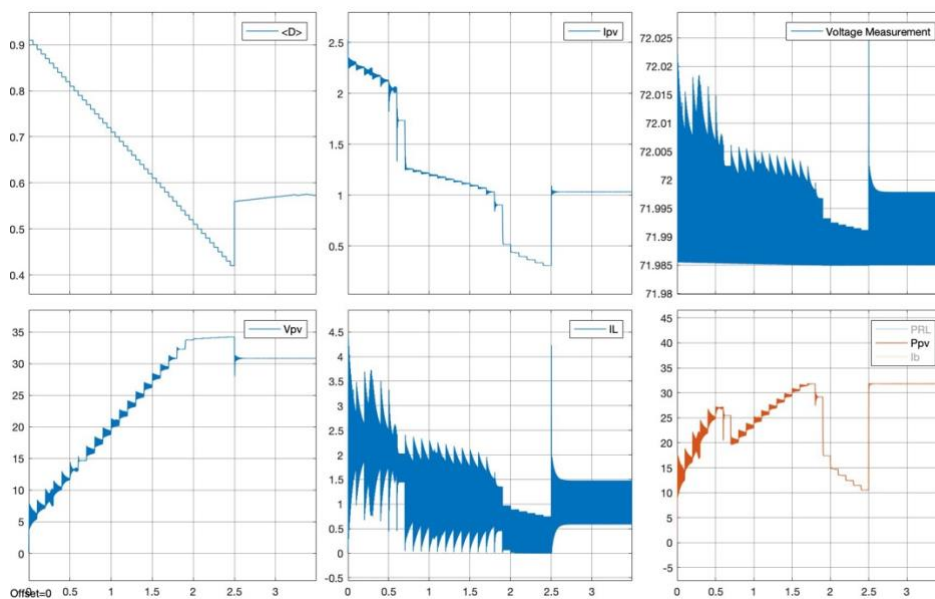


Figure 6.26: Simulation of Duty Sweeping algorithm

As it can be observed in the previous figure, almost all the P-V curve is analyzed by the controller (except its extrema as D is swept from 0.915 to 0.415) and all of its corresponding D , V_{pv} and P_{pv} are stored.

As a result, the system can identify the absolute maximum power point, 32W, (with $D=0.57$ and $V_{pv}=31V$), setting it as the operating point and, carry out P&O around it.

The response of this method to a change in the irradiance conditions has also been studied. For the first 3.5 seconds of the simulation the irradiance received by each panel is $1000W/m^2$ and afterwards, the irradiance in the second panel decreases to $500W/m^2$:

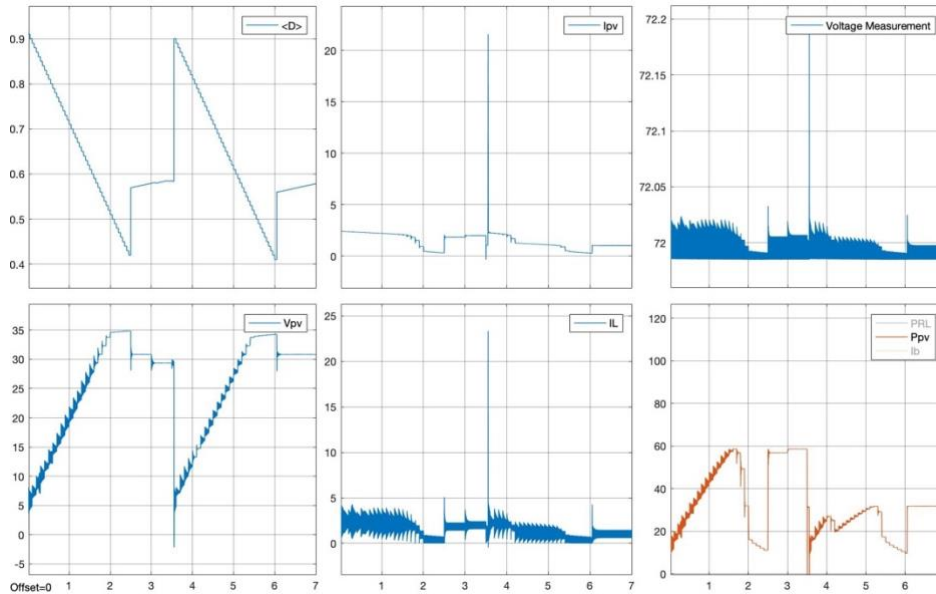


Figure 6.27: Simulation of Duty Sweeping algorithm with a change in irradiance

So, during first 2 seconds of the simulation, the controller carries out a sweeping from $D=0.9$ to $D=0.4$ of the curve at $1000\text{W}/\text{m}^2$. This curve has its maximum power at 58W , and it only has one maximum because the irradiance is the same in both panels of the array. Next, the MPP is detected and set as operation point and P&O starts to work to maintain the power around that point ($D=0.59$, $V_{pv}=29\text{V}$, $P_{pv}=58\text{W}$).

When the change in irradiance is introduced, the system detects a decrease in the power extracted from the panels with respect to the previous value greater than 10% so it carries out Duty Sweeping again. In this case there are two peaks of power, but the system can detect the absolute maximum and set it as operation point ($D=0.58$, $V_{pv}=31\text{V}$, $P_{pv}=32\text{W}$).

For the Duty Sweeping algorithm case, the efficiency of the regulator is:

$$\eta = \frac{P_{out}}{V_{pv} \cdot I_{pv}} \cdot 100 \approx \frac{32}{31 \cdot 1.1} \cdot 100 = 93.84\% \quad (eq. 17)$$

The previous simulations of the load regulator with P&O and Duty Sweeping are repeated with a change in the frequency of the PWM pulse generator (initially 10KHz). It is tested with 20KHz and 1000Hz . With 20KHz , the result is the same as with 10KHz ; however, with 1000Hz , the behavior of the system changes completely: the variation of the duty cycle is carried out properly, but the signals recorded (V_{pv} and I_{pv}) have large oscillations. This makes the controller take as values of power, values which are not

realistic (they can be the ones in the peak of an oscillation and not the mean values) and then and the real maximum power point is not reached.

If it was desired to work with a low frequency controller in a real implementation of this load regulator, the sampling time of the system would need to be increased in order to leave enough time for the signals to stabilize between one sampling and another. Depending on the type of microcontroller used, a higher sampling time could also be a constraint as it may get slower and lose the pace of sampling.

solution could be using a filter in the sensing of current and voltage to soften the irregularities of these variables.

7. CONCLUSIONS

Concerning the study of the 4 photovoltaic panels available in the laboratory of Mechanics, the following conclusions arise:

- I. After having measured the working parameters of the four panels under study, it has been proved that their electric characteristics are similar. Consequently, they can be arranged together to form a photovoltaic array without the risk of having unequal behavior among them. There were some irregularities among their measured parameters, but they were probably caused the variability of the conditions and by the lack of accuracy in the measurements. Moreover, their characteristics parameters V_{oc} , I_{sc} , P_{max} and V and I at P_{max} have been deduced to implement them in the load regulator's simulation.
- II. The calculated I-V and P-V curves under PSC have a similar shape to the theoretical ones in rough outlines. However, due to the connections or the imprecision at measuring, some differences are observed.
- III. The increase in the ambient temperature has a negative effect in the working parameters of the P-V panels. When the ambient temperature is around 25°C and the irradiance 900 W/m², the cells reach a temperature of 40° (approximately) which is the temperature from which the efficiency of the panels starts to decrease.

When temperature reaches this value, both in the short circuit current and in the open circuit voltage of the panel as they are both reduced.

Regarding the commercial load regulator studied:

- I. When the power extracted from the PV-panels is sufficient to feed the load, the load is fed, and the battery is charged. When the power from the panels is not enough to feed the load with the requested power, the batteries contribute too to feeding the load and they are discharged.
- II. The regulator available in the laboratory was not able to extract the maximum power available under PSC. Consequently, it can be deduced that the MPPT technique used in its microcontroller is not one capable of working under PSC.

Concerning the design and simulation of a load regulator to carry out the MPPT of a PV-array and feed a load or a battery:

- I. The sampling and switching frequency of the microcontroller, the value of the inductance L and the variation of the duty cycle are determinant parameters in the simulation of the load regulator in MATLAB/Simulink. If they are not properly defined, the simulation may show an incorrect behavior of the photovoltaic system.
- II. The value calculated for the C_{out} was to limit the ripple at the output but the values still vary above the expected values (above the 1% computed).
- III. The regulator's time response determines the sampling time of the controller and this requires much time to produce the simulation. In a real system this period of time can be in the range of seconds. This is even more important when the duty sweeping procedure is used as it requires waiting for the system response to each applied value of D set by the controller.

IV. When the PV-panels are under constant irradiance conditions, both P&O and Duty Sweeping algorithms work properly. However, under PSC, P&O method is only capable of reaching the local maximum power closer to the initial point set in the curve. Duty sweeping method, as it studies and stores all the power and D values of the curve, can select always the absolute maximum power point in the curve.

Duty Sweeping method is also able of detecting changes in the irradiance conditions and start a new sweeping procedure to define the new optimal operation point. On the downside, duty sweeping algorithm requires memory space for storing the power and D values and its convergence towards the RMPP point will depend on the number of points taken and on the system time constant. It also has a lower efficiency than the P&O method.

V. Regarding the frequency at which the controller of the load regulator should work: the frequencies that have worked properly in the simulations are 10KHz and 20KHz; consequently, a microcontroller capable of working at high frequencies is required (i. e. a DSP microcontroller). If we wanted to use a lower frequency microcontroller like an Arduino, then the sampling time and variation of parameter D would require modifications and filters at the sensed variables may be needed.

As a general conclusion, it can be stated that the proposed objectives have been achieved. The simulation of a photovoltaic system under PSC which could be implemented in the surface of a vehicle has been fulfilled. The panel models used in the simulation had the characteristics measured from the panels of the Mechanical Engineering department and two MPPT algorithms have been simulated and compared working with the load regulator.

Several difficulties have raised in the measurements with the PV-panels and in the work done in the simulations with MATLAB/Simulink. However, the knowledge acquired on these fields is extensive and extremely valuable for my future academic development.

Future issues of study of this work would be the following ones:

- i. The physical design and implementation of the proposed system and checking of its operation.
- ii. The study of the influence of the regulator and controller's parameters in the presence of a different PV-array configuration (more than 2 panels in series or more strings in parallel).
- iii. The design of a MPPT algorithm based on the approximated characteristic curves obtained experimentally. The information of the curves could be used to take faster decisions; however, a pyranometer should be used at every time.

8. BIBLIOGRAPHY AND REFERENCES

- [1] European Environment Agency, “Transport”, March 2020 [Online]. Available: <https://www.eea.europa.eu/themes/transport/intro>.
- [2] L. M. Marroyo and J. Marcos, “Convertidores Electrónicos de Potencia”, UPNA, Pamplona, 2020.
- [3] C.-Y. Tang, S.-H. Lin and S.-Y. Ou, "Design and implementation of a hybrid maximum power point tracker in solar power system under partially shaded conditions," 2017 IEEE 3rd International Future Energy Electronics Conference and ECCE Asia (IFEEEC 2017 - ECCE Asia), 2017, pp. 900-905, doi: 10.1109/IFEEEC.2017.7992160.
- [4] A. Ursúa, “Energías Renovables”, UPNA, Pamplona, 2020.
- [5] S. Pindado, J. Cubas & C. Manuel, “Explicit Expressions for Solar Panel Equivalent Circuit Parameters Based on Analytical Formulation and the Lambert W-Function”, *Energies*. 7. 4098-4115. 10.3390/en7074098, 2014.
- [6] R. F. Coelho, F. Concer and D. C. Martins, “A study of the basic DC-DC converters applied in maximum power point tracking,” *IEEE Power Electronics Conf.*,2009, pp.673 –678, Brazil.
- [7] I. Glasner and J. Appelbaum, “Advantage of boost vs. buck topology for maximum power point tracker in photovoltaic systems,” *Electrical and Electronics Engineers in Israel*, pp. 355-358, 1996.
- [8] T. Eswam and P. L. Chapman, “Comparison of photovoltaic array maximum power point tracking techniques,” *IEEE Trans. Energy Conversion.*, vol.22, no.2, pp.439–449, June 2007.

- [9] C.-Y. Won, D.-H. Kim, S.-C. Kim, W.-S. Kim, and H.-S. Kim, “A new maximum power point tracker of photovoltaic arrays using fuzzy controller,” in *Proc. 25th Annu. IEEE Power Electron. Spec. Conf.*, 1994, pp. 396–403.
- [10] D. Shmilovitz, “On the control of photovoltaic maximum power point tracker via output parameters,” *IEE Proc. Elect. Power Appl.*, 2005, pp. 239–248.
- [11] P. Weng, “DC-DC Boost Converter with Constant Output Voltage for Grid”, EEPIS repository, 2010.

ÉLIDA MENDIETA IRISARRI

Faro, July 2021

APPENDIX

APPENDIX 1

MEASUREMENT OF THE PANELS' PARAMETERS

For each panel, all the data recorded for a close range of irradiance is arranged together to draw the characteristic curves of each panel.

Table A.1: data recorded for panel A

| PANEL A | | | | | | |
|---------|-------|--------------------------|-----------------------------------|----------------|----------------|--------------|
| DATE | TIME | T _{sup} (°C) | IRRADIANCE (W/m ²) | VOLTAGE (V) | CURRENT (A) | POWER (W) |
| 9/3/21 | 16:16 | 26.20 | 98.00 | 18.82 | 0.00 | 0 |
| 9/3/21 | 16:15 | 26.10 | 98.30 | 11.46 | 0.30 | 3.46092 |
| 9/3/21 | 16:15 | 26.10 | 98.30 | 11.65 | 0.29 | 3.3319 |
| 9/3/21 | 16:15 | 26.40 | 98.30 | 12.57 | 0.30 | 3.771 |
| 9/3/21 | 16:14 | 26.20 | 100.40 | 9.24 | 0.31 | 2.84592 |
| 9/3/21 | 16:14 | 25.80 | 100.40 | 10.18 | 0.30 | 3.09472 |
| 9/3/21 | 16:14 | 26.10 | 100.40 | 10.81 | 0.30 | 3.27543 |
| 9/3/21 | 16:11 | 26.20 | 100.70 | 5.74 | 0.26 | 1.51536 |
| 9/3/21 | 16:11 | 26.40 | 100.70 | 6.44 | 0.31 | 2.01572 |
| 9/3/21 | 16:12 | 26.10 | 100.70 | 6.58 | 0.31 | 2.03322 |
| 9/3/21 | 16:12 | 25.80 | 100.70 | 7.11 | 0.31 | 2.2041 |
| 9/3/21 | 16:13 | 25.70 | 100.70 | 8.23 | 0.31 | 2.53484 |
| 9/3/21 | 16:13 | 25.30 | 100.70 | 8.97 | 0.31 | 2.76276 |
| 9/3/21 | 16:10 | 25.60 | 101.90 | 4.60 | 0.32 | 1.458834 |
| 9/3/21 | 16:10 | 26.40 | 101.90 | 5.26 | 0.32 | 1.65564 |
| 9/3/21 | 16:00 | 27.00 | 109.60 | 2.76 | 0.34 | 0.935979 |
| 9/3/21 | 16:00 | 26.70 | 109.60 | 3.51 | 0.34 | 1.181185 |
| 9/3/21 | 16:01 | 26.70 | 109.60 | 4.12 | 0.34 | 1.383984 |
| 9/3/21 | 15:59 | 27.30 | 110.80 | 1.46 | 0.35 | 0.506688 |
| 9/3/21 | 15:59 | 26.90 | 110.80 | 2.09 | 0.34 | 0.70958 |

STUDY ON PARTIALLY SHADED CONDITIONS REGULATORS FOR PV BASED ELECTRICALLY POWERED VEHICLES

| | | | | | | |
|--------|-------|-------|--------|-------|------|----------|
| 9/3/21 | 15:58 | 27.50 | 112.90 | 0.08 | 0.35 | 0.02622 |
| 9/3/21 | 15:58 | 27.70 | 112.90 | 0.71 | 0.35 | 0.248139 |
| 8/3/21 | 15:08 | 36.20 | 188.00 | 18.30 | 0.00 | 0 |
| 8/3/21 | 14:57 | 30.90 | 221.90 | 15.32 | 0.50 | 7.61404 |
| 9/3/21 | 14:31 | 22.10 | 222.50 | 16.88 | 0.40 | 6.78576 |
| 9/3/21 | 14:31 | 22.50 | 223.00 | 18.99 | 0.00 | 0 |
| 8/3/21 | 14:56 | 30.40 | 226.10 | 14.37 | 0.49 | 7.07004 |
| 9/3/21 | 14:30 | 23.90 | 232.80 | 16.29 | 0.45 | 7.37937 |
| 9/3/21 | 14:30 | 23.30 | 232.80 | 16.50 | 0.43 | 7.161 |
| 9/3/21 | 14:30 | 22.50 | 232.80 | 16.69 | 0.42 | 6.97642 |
| 8/3/21 | 14:58 | 31.10 | 250.90 | 16.25 | 0.50 | 8.0925 |
| 8/3/21 | 14:51 | 36.80 | 367.40 | 17.69 | 0.78 | 13.85127 |
| 3/3/21 | 16:30 | 31.00 | 404.10 | 1.69 | 1.12 | 1.894467 |
| 3/3/21 | 16:30 | 31.10 | 404.10 | 0.17 | 1.12 | 0.190836 |
| 3/3/21 | 16:29 | 30.90 | 412.30 | 8.96 | 1.12 | 10.05312 |
| 3/3/21 | 16:29 | 31.50 | 412.30 | 6.53 | 1.12 | 7.30054 |
| 3/3/21 | 16:29 | 31.50 | 412.30 | 3.87 | 1.12 | 4.32992 |
| 3/3/21 | 16:27 | 31.70 | 423.60 | 16.43 | 0.87 | 14.22838 |
| 3/3/21 | 16:27 | 30.90 | 423.60 | 15.83 | 0.94 | 14.92769 |
| 3/3/21 | 16:28 | 31.30 | 423.60 | 15.04 | 1.02 | 15.28064 |
| 3/3/21 | 16:28 | 31.40 | 423.60 | 13.68 | 1.08 | 14.78808 |
| 3/3/21 | 16:28 | 31.00 | 423.60 | 11.51 | 1.11 | 12.78761 |
| 3/3/21 | 16:26 | 30.80 | 430.90 | 16.84 | 0.80 | 13.48884 |
| 3/3/21 | 14:32 | 38.40 | 524.90 | 5.57 | 1.47 | 8.172657 |
| 3/3/21 | 14:32 | 37.60 | 524.90 | 1.60 | 1.50 | 2.4032 |
| 8/3/21 | 15:00 | 31.40 | 567.60 | 18.90 | 0.48 | 9.1098 |
| 3/3/21 | 14:25 | 39.60 | 608.80 | 17.03 | 0.82 | 13.93054 |
| 3/3/21 | 14:25 | 38.30 | 608.80 | 16.88 | 0.89 | 15.05696 |
| 3/3/21 | 14:30 | 39.30 | 620.40 | 11.96 | 1.45 | 17.2822 |
| 3/3/21 | 14:33 | 37.80 | 620.40 | 0.29 | 1.49 | 0.43659 |
| 3/3/21 | 14:31 | 39.40 | 623.80 | 8.58 | 1.47 | 12.57828 |
| 3/3/21 | 14:26 | 39.50 | 634.50 | 16.50 | 0.98 | 16.1865 |

STUDY ON PARTIALLY SHADED CONDITIONS REGULATORS FOR PV BASED ELECTRICALLY POWERED VEHICLES

| | | | | | | |
|--------|-------|-------|--------|-------|------|----------|
| 3/3/21 | 14:26 | 39.30 | 634.50 | 15.97 | 0.92 | 14.6924 |
| 8/3/21 | 14:54 | 35.20 | 662.50 | 18.12 | 0.68 | 12.24912 |
| 9/3/21 | 15:43 | 46.50 | 668.00 | 17.99 | 0.48 | 8.56324 |
| 9/3/21 | 15:44 | 46.80 | 668.30 | 18.03 | 0.45 | 8.13153 |
| 9/3/21 | 15:44 | 46.60 | 668.30 | 18.08 | 0.43 | 7.75632 |
| 9/3/21 | 15:44 | 46.50 | 668.30 | 18.98 | 0.00 | 0 |
| 9/3/21 | 15:42 | 46.20 | 673.20 | 17.89 | 0.53 | 9.49959 |
| 9/3/21 | 15:42 | 46.50 | 673.20 | 17.94 | 0.50 | 9.00588 |
| 9/3/21 | 15:41 | 46.20 | 673.80 | 17.83 | 0.56 | 10.00263 |
| 9/3/21 | 15:40 | 46.00 | 675.00 | 17.60 | 0.65 | 11.3696 |
| 9/3/21 | 15:40 | 46.00 | 675.00 | 17.73 | 0.60 | 10.62027 |
| 9/3/21 | 15:39 | 45.60 | 679.60 | 17.35 | 0.76 | 13.20335 |
| 9/3/21 | 15:39 | 45.70 | 679.60 | 17.49 | 0.70 | 12.19053 |
| 9/3/21 | 15:37 | 45.10 | 684.50 | 15.53 | 1.24 | 19.27273 |
| 9/3/21 | 15:38 | 44.60 | 684.80 | 16.93 | 0.90 | 15.27086 |
| 9/3/21 | 15:38 | 44.90 | 684.80 | 17.16 | 0.83 | 14.29428 |
| 9/3/21 | 15:37 | 44.80 | 685.00 | 16.19 | 1.10 | 17.87376 |
| 9/3/21 | 15:37 | 44.70 | 685.00 | 16.60 | 1.00 | 16.5834 |
| 9/3/21 | 15:35 | 45.20 | 687.60 | 12.95 | 1.53 | 19.7876 |
| 9/3/21 | 15:36 | 45.30 | 687.60 | 14.64 | 1.38 | 20.18856 |
| 9/3/21 | 15:34 | 44.50 | 688.50 | 7.22 | 1.59 | 11.45814 |
| 9/3/21 | 15:34 | 44.90 | 688.50 | 9.76 | 1.57 | 15.3232 |
| 8/3/21 | 14:42 | 24.60 | 735.20 | 8.48 | 2.43 | 20.564 |
| 8/3/21 | 14:52 | 36.80 | 757.10 | 17.77 | 0.71 | 12.56339 |
| 9/3/21 | 14:19 | 33.80 | 897.80 | 0.48 | 2.44 | 1.17216 |
| 9/3/21 | 14:21 | 33.80 | 910.00 | 12.87 | 2.16 | 27.82494 |
| 9/3/21 | 14:20 | 34.00 | 910.60 | 3.44 | 2.39 | 8.228178 |
| 8/3/21 | 15:04 | 37.40 | 911.90 | 19.33 | 0.00 | 0 |
| 8/3/21 | 15:01 | 32.20 | 916.40 | 19.49 | 0.49 | 9.45265 |
| 8/3/21 | 15:01 | 34.40 | 916.40 | 19.47 | 0.49 | 9.44295 |
| 8/3/21 | 14:45 | 29.10 | 927.10 | 17.89 | 1.41 | 25.17123 |
| 8/3/21 | 14:44 | 27.30 | 929.30 | 17.30 | 1.67 | 28.8391 |

STUDY ON PARTIALLY SHADED CONDITIONS REGULATORS FOR PV BASED ELECTRICALLY POWERED VEHICLES

| | | | | | | |
|--------|-------|-------|--------|-------|------|----------|
| 8/3/21 | 14:46 | 30.80 | 933.80 | 18.15 | 1.22 | 22.0704 |
| 8/3/21 | 14:46 | 31.30 | 933.80 | 18.42 | 1.07 | 19.7094 |
| 8/3/21 | 14:46 | 32.20 | 933.80 | 18.54 | 0.97 | 17.94672 |
| 8/3/21 | 15:02 | 35.10 | 957.30 | 19.04 | 0.43 | 8.24432 |
| 8/3/21 | 14:43 | 25.40 | 958.10 | 15.58 | 2.03 | 31.58066 |

Table A.2: data recorded for panel B

| PANEL B | | | | | | |
|---------|-------|--------------|-----------------------------------|----------------|----------------|--------------|
| DATE | TIME | Tsup (°C) | IRRADIANCE (W/m ²) | VOLTAGE (V) | CURRENT (A) | POWER (W) |
| 9/3/21 | 16:28 | 21.2 | 88.5 | 18.56 | 0 | 0 |
| 9/3/21 | 16:27 | 21.7 | 89.4 | 8.84 | 0.264 | 2.33376 |
| 9/3/21 | 16:27 | 21.3 | 89.4 | 9.83 | 0.262 | 2.57546 |
| 9/3/21 | 16:26 | 21.9 | 90.6 | 6.83 | 0.269 | 1.83727 |
| 9/3/21 | 16:25 | 22.7 | 91.6 | 5.77 | 0.274 | 1.58098 |
| 9/3/21 | 16:25 | 22.2 | 91.6 | 6.24 | 0.271 | 1.69104 |
| 9/3/21 | 16:24 | 23.9 | 92.2 | 5.208 | 0.277 | 1.442616 |
| 8/3/21 | 15:48 | 21.4 | 92.5 | 7.63 | 0.244 | 1.86172 |
| 9/3/21 | 16:20 | 24.7 | 92.5 | 0.044 | 0.288 | 0.012672 |
| 9/3/21 | 16:21 | 24.4 | 92.5 | 0.528 | 0.284 | 0.149952 |
| 9/3/21 | 16:21 | 24.5 | 92.5 | 1.11 | 0.284 | 0.31524 |
| 9/3/21 | 16:21 | 24.3 | 92.5 | 1.682 | 0.275 | 0.46255 |
| 9/3/21 | 16:23 | 24.3 | 93.4 | 3.467 | 0.283 | 0.981161 |
| 9/3/21 | 16:23 | 24.4 | 93.4 | 4.02 | 0.281 | 1.12962 |
| 9/3/21 | 16:23 | 24.4 | 93.4 | 4.662 | 0.28 | 1.30536 |
| 9/3/21 | 16:22 | 24.4 | 93.7 | 2.191 | 0.281 | 0.615671 |
| 9/3/21 | 16:22 | 24.5 | 93.7 | 2.842 | 0.284 | 0.807128 |
| 8/3/21 | 15:46 | 21.8 | 105 | 18.59 | 0 | 0 |
| 8/3/21 | 15:45 | 22 | 111.7 | 11.32 | 0.268 | 3.03376 |
| 8/3/21 | 15:45 | 22.6 | 115.7 | 10.72 | 0.28 | 3.0016 |
| 8/3/21 | 15:44 | 23 | 125.1 | 5.32 | 0.311 | 1.65452 |
| 9/3/21 | 14:34 | 33.4 | 238 | 6.73 | 0.972 | 6.54156 |

STUDY ON PARTIALLY SHADED CONDITIONS REGULATORS FOR PV BASED ELECTRICALLY POWERED VEHICLES

| | | | | | | |
|---------|-------|------|-------|-------|-------|----------|
| 9/3/21 | 14:34 | 33.4 | 238 | 6.73 | 0.972 | 6.54156 |
| 8/3/21 | 15:36 | 27.3 | 298.5 | 9.12 | 1.02 | 9.3024 |
| 3/3/21 | 16:33 | 30.8 | 388.2 | 13.66 | 0.925 | 12.6355 |
| 3/3/21 | 16:33 | 30.3 | 388.2 | 12.02 | 0.955 | 11.4791 |
| 3/3/21 | 16:33 | 29.6 | 388.2 | 10.12 | 0.967 | 9.78604 |
| 3/3/21 | 16:32 | 31.3 | 391.5 | 16.05 | 0.772 | 12.3906 |
| 3/3/21 | 16:32 | 30.6 | 391.5 | 15.58 | 0.821 | 12.79118 |
| 3/3/21 | 16:32 | 30.5 | 391.5 | 14.81 | 0.875 | 12.95875 |
| 2/3/21 | 15:45 | 27.3 | 392.2 | 1.304 | 0.895 | 1.16708 |
| 3/3/21 | 16:34 | 29.3 | 392.5 | 7.87 | 0.97 | 7.6339 |
| 8/3/21 | 15:33 | 27.7 | 569.5 | 19.12 | 0 | 0 |
| 9/3/21 | 14:45 | 38.4 | 592 | 18.11 | 0.449 | 8.13139 |
| 3/3/21 | 14:42 | 39.6 | 610.4 | 2.452 | 1.461 | 3.582372 |
| 3/3/21 | 14:42 | 39.6 | 610.4 | 0.433 | 1.644 | 0.711852 |
| 3/3/21 | 14:36 | 41.9 | 610.7 | 16.51 | 0.791 | 13.05941 |
| 3/3/21 | 14:36 | 41.6 | 610.7 | 16.28 | 0.867 | 14.11476 |
| 3/3/21 | 14:37 | 40.5 | 621.3 | 16.01 | 0.95 | 15.2095 |
| 3/3/21 | 14:37 | 41.2 | 621.3 | 15.53 | 1.042 | 16.18226 |
| 3/3/21 | 14:38 | 40.7 | 621.6 | 14.87 | 1.152 | 17.13024 |
| 3/3/21 | 14:39 | 40.4 | 624.7 | 13.69 | 1.228 | 16.81132 |
| 3/3/21 | 14:39 | 40.1 | 624.7 | 10.52 | 1.357 | 14.27564 |
| 3/3/21 | 14:40 | 39.8 | 624.7 | 8.48 | 1.445 | 12.2536 |
| 15/3/21 | 14:38 | 42.4 | 847.8 | 0.422 | 2.073 | 0.874806 |
| 15/3/21 | 14:39 | 44 | 854.5 | 3.238 | 2.072 | 6.709136 |
| 15/3/21 | 14:39 | 43.2 | 854.5 | 7.04 | 2.07 | 14.5728 |
| 15/3/21 | 14:39 | 43.3 | 854.5 | 11.34 | 2.007 | 22.75938 |
| 15/3/21 | 14:40 | 43.9 | 857.5 | 13.89 | 1.799 | 24.98811 |
| 15/3/21 | 14:40 | 42.3 | 857.5 | 15.31 | 1.524 | 23.33244 |
| 15/3/21 | 14:40 | 42.2 | 857.5 | 16.16 | 1.29 | 20.8464 |
| 15/3/21 | 14:41 | 42.7 | 857.8 | 16.18 | 1.291 | 20.88838 |
| 15/3/21 | 14:41 | 42.4 | 857.8 | 16.68 | 1.118 | 18.64824 |
| 15/3/21 | 14:41 | 43.4 | 857.8 | 16.99 | 0.994 | 16.88806 |

STUDY ON PARTIALLY SHADED CONDITIONS REGULATORS FOR PV BASED ELECTRICALLY POWERED VEHICLES

| | | | | | | |
|---------|-------|------|-------|-------|-------|----------|
| 15/3/21 | 14:42 | 40.9 | 859.4 | 17.41 | 0.825 | 14.36325 |
| 15/3/21 | 14:43 | 42.8 | 857.2 | 17.49 | 0.772 | 13.50228 |
| 15/3/21 | 14:43 | 42.1 | 857.2 | 17.68 | 0.716 | 12.65888 |
| 15/3/21 | 14:44 | 43.3 | 850.8 | 17.77 | 0.664 | 11.79928 |
| 15/3/21 | 14:44 | 43.9 | 850.8 | 17.85 | 0.62 | 11.067 |
| 15/3/21 | 14:45 | 44.5 | 842.9 | 17.91 | 0.581 | 10.40571 |
| 15/3/21 | 14:45 | 45.2 | 842.9 | 17.96 | 0.533 | 9.57268 |
| 15/3/21 | 14:45 | 44.9 | 842.9 | 17.99 | 0.499 | 8.97701 |
| 15/3/21 | 14:46 | 44.1 | 832.5 | 18.03 | 0.47 | 8.4741 |
| 15/3/21 | 14:46 | 43.8 | 832.5 | 18.07 | 0.449 | 8.11343 |
| 15/3/21 | 14:47 | 44.3 | 811.8 | 18.09 | 0.427 | 7.72443 |
| 15/3/21 | 14:47 | 44.2 | 811.8 | 18.81 | 0 | 0 |

Table A.3: data recorded for panel C

| PANEL C | | | | | | |
|---------|-------|--------------|----------------------|----------------|----------------|--------------|
| DATE | TIME | Tsup (°C) | IRRADIANCE (W/m2) | VOLTAGE (V) | CURRENT (A) | POWER (W) |
| 9/3/21 | 16:36 | 20.7 | 84.8 | 19.49 | 0 | 0 |
| 9/3/21 | 16:34 | 20.7 | 85.1 | 6.2 | 0.249 | 1.5438 |
| 9/3/21 | 16:34 | 20.5 | 85.1 | 7.2 | 0.246 | 1.7712 |
| 9/3/21 | 16:35 | 20.5 | 85.4 | 8.15 | 0.244 | 1.9886 |
| 9/3/21 | 16:35 | 20.7 | 85.4 | 9.15 | 0.242 | 2.2143 |
| 9/3/21 | 16:35 | 20.8 | 85.4 | 10.17 | 0.24 | 2.4408 |
| 9/3/21 | 16:33 | 20.8 | 86.1 | 4.205 | 0.254 | 1.06807 |
| 9/3/21 | 16:33 | 20.7 | 86.1 | 5.382 | 0.252 | 1.356264 |
| 9/3/21 | 16:31 | 20.9 | 86.4 | 0.042 | 0.264 | 0.011088 |
| 9/3/21 | 16:31 | 20.9 | 86.4 | 1.054 | 0.262 | 0.276148 |
| 9/3/21 | 16:32 | 21 | 86.4 | 2.113 | 0.258 | 0.545154 |
| 9/3/21 | 16:32 | 21.1 | 86.4 | 3.182 | 0.255 | 0.81141 |
| 3/3/21 | 16:23 | 30.6 | 449.5 | 6.62 | 1.11 | 7.3482 |
| 3/3/21 | 16:23 | 30.3 | 449.5 | 4.135 | 1.124 | 4.64774 |
| 3/3/21 | 16:20 | 32 | 457.2 | 16.33 | 0.764 | 12.47612 |

STUDY ON PARTIALLY SHADED CONDITIONS REGULATORS FOR PV BASED ELECTRICALLY POWERED VEHICLES

| | | | | | | |
|---------|-------|------|-------|-------|-------|----------|
| 3/3/21 | 16:20 | 31.8 | 457.2 | 15.83 | 0.829 | 13.12307 |
| 3/3/21 | 16:22 | 31.5 | 457.8 | 13.27 | 1.047 | 13.89369 |
| 3/3/21 | 16:22 | 31.3 | 457.8 | 11.18 | 1.078 | 12.05204 |
| 3/3/21 | 16:22 | 30.6 | 457.8 | 8.99 | 1.096 | 9.85304 |
| 3/3/21 | 16:21 | 32.5 | 464.8 | 15.27 | 0.909 | 13.88043 |
| 3/3/21 | 16:21 | 32.2 | 464.8 | 14.58 | 0.971 | 14.15718 |
| 3/3/21 | 15:13 | 31.7 | 538.3 | 2.675 | 1.275 | 3.410625 |
| 3/3/21 | 15:13 | 31.1 | 538.3 | 0.222 | 1.303 | 0.289266 |
| 3/3/21 | 15:12 | 31.3 | 541.4 | 7.36 | 1.234 | 9.08224 |
| 3/3/21 | 15:12 | 30.7 | 541.4 | 5.107 | 1.264 | 6.455248 |
| 3/3/21 | 15:10 | 32.4 | 542.3 | 15.19 | 0.903 | 13.71657 |
| 3/3/21 | 15:10 | 32.3 | 542.3 | 14.49 | 0.988 | 14.31612 |
| 3/3/21 | 15:10 | 31.9 | 542.3 | 13.54 | 1.078 | 14.59612 |
| 3/3/21 | 15:09 | 31.7 | 549.3 | 16.07 | 0.768 | 12.34176 |
| 3/3/21 | 15:09 | 32.2 | 549.3 | 15.7 | 0.832 | 13.0624 |
| 9/3/21 | 15:06 | 44.8 | 723.6 | 18.95 | 0 | 0 |
| 9/3/21 | 15:05 | 47.7 | 725.7 | 17.94 | 0.452 | 8.10888 |
| 9/3/21 | 15:05 | 47.1 | 726 | 17.99 | 0.427 | 7.68173 |
| 9/3/21 | 15:04 | 47.7 | 730.3 | 17.78 | 0.498 | 8.85444 |
| 9/3/21 | 15:04 | 47.6 | 730.3 | 17.85 | 0.474 | 8.4609 |
| 9/3/21 | 15:04 | 47.7 | 730.3 | 17.78 | 0.498 | 8.85444 |
| 9/3/21 | 15:04 | 47.6 | 730.3 | 17.85 | 0.474 | 8.4609 |
| 15/3/21 | 14:50 | 43.2 | 784.6 | 0.23 | 2.08 | 0.4784 |
| 15/3/21 | 14:50 | 43.7 | 784.6 | 2.473 | 1.996 | 4.936108 |
| 15/3/21 | 14:50 | 44 | 784.6 | 6.57 | 1.923 | 12.63411 |
| 15/3/21 | 14:50 | 43 | 784.6 | 10.32 | 1.854 | 19.13328 |
| 15/3/21 | 14:51 | 42.1 | 770.3 | 12.94 | 1.678 | 21.71332 |
| 15/3/21 | 14:51 | 43 | 764.8 | 14.32 | 1.469 | 21.03608 |
| 15/3/21 | 14:52 | 42.6 | 764.8 | 15.44 | 1.241 | 19.16104 |
| 15/3/21 | 14:52 | 42.7 | 764.8 | 15.91 | 1.125 | 17.89875 |
| 15/3/21 | 14:52 | 42.8 | 764.8 | 16.49 | 0.964 | 15.89636 |
| 15/3/21 | 14:53 | 40.8 | 760.8 | 16.75 | 0.888 | 14.874 |

STUDY ON PARTIALLY SHADED CONDITIONS REGULATORS FOR PV BASED ELECTRICALLY POWERED VEHICLES

| | | | | | | |
|---------|-------|------|-------|-------|-------|----------|
| 15/3/21 | 14:53 | 42.7 | 760.8 | 17.03 | 0.803 | 13.67509 |
| 15/3/21 | 14:55 | 43.1 | 746.5 | 17.1 | 0.806 | 13.7826 |
| 15/3/21 | 14:56 | 43 | 741.6 | 17.23 | 0.763 | 13.14649 |
| 15/3/21 | 14:56 | 42.6 | 741.6 | 17.41 | 0.707 | 12.30887 |
| 15/3/21 | 14:56 | 43 | 741.6 | 17.69 | 0.618 | 10.93242 |
| 15/3/21 | 14:57 | 42.8 | 743.1 | 17.8 | 0.574 | 10.2172 |
| 15/3/21 | 14:57 | 43.3 | 743.1 | 17.9 | 0.537 | 9.6123 |
| 15/3/21 | 14:57 | 43 | 743.1 | 18 | 0.502 | 9.036 |
| 15/3/21 | 14:58 | 43.2 | 752.9 | 18.07 | 0.476 | 8.60132 |
| 15/3/21 | 14:58 | 43.7 | 752.9 | 18.11 | 0.477 | 8.63847 |
| 15/3/21 | 14:58 | 43.4 | 752.9 | 18.16 | 0.429 | 7.79064 |
| 15/3/21 | 14:59 | 43.4 | 749.2 | 19.13 | 0 | 0 |

Table A.4: data recorded for panel D

| PANEL D | | | | | | |
|---------|-------|--------------|----------------------|----------------|----------------|--------------|
| DATE | TIME | Tsup (°C) | IRRADIANCE (W/m2) | VOLTAGE (V) | CURRENT (A) | POWER (W) |
| 9/3/21 | 16:44 | 20.2 | 79.3 | 8.23 | 0.219 | 1.80237 |
| 9/3/21 | 16:44 | 20.1 | 79.3 | 9.21 | 0.217 | 1.99857 |
| 9/3/21 | 16:44 | 20.1 | 79.3 | 18.91 | 0 | 0 |
| 9/3/21 | 16:43 | 20.1 | 80.6 | 6.48 | 0.222 | 1.43856 |
| 9/3/21 | 16:43 | 20.3 | 80.6 | 7.3 | 0.218 | 1.5914 |
| 9/3/21 | 16:41 | 20.5 | 81.8 | 5.593 | 0.221 | 1.236053 |
| 9/3/21 | 16:41 | 20.5 | 81.8 | 6.41 | 0.222 | 1.42302 |
| 9/3/21 | 16:39 | 21.3 | 82.7 | 0.931 | 0.238 | 0.221578 |
| 9/3/21 | 16:39 | 20.9 | 82.7 | 1.938 | 0.233 | 0.451554 |
| 9/3/21 | 16:40 | 20.7 | 82.7 | 2.911 | 0.231 | 0.672441 |
| 9/3/21 | 16:40 | 20.8 | 82.7 | 3.804 | 0.229 | 0.871116 |
| 9/3/21 | 16:38 | 21.1 | 83.3 | 0.038 | 0.24 | 0.00912 |
| 2/3/21 | 16:09 | 23.5 | 296.9 | 0.076 | 0.744 | 0.056544 |
| 2/3/21 | 16:09 | 23.5 | 298.2 | 1.69 | 0.743 | 1.25567 |
| 2/3/21 | 16:08 | 23.2 | 299.7 | 2.785 | 0.722 | 2.01077 |

STUDY ON PARTIALLY SHADED CONDITIONS REGULATORS FOR PV BASED ELECTRICALLY POWERED VEHICLES

| | | | | | | |
|--------|-------|------|-------|-------|-------|----------|
| 2/3/21 | 16:07 | 23 | 301.5 | 4.375 | 0.714 | 3.12375 |
| 2/3/21 | 16:07 | 23.1 | 302.1 | 5.78 | 0.717 | 4.14426 |
| 2/3/21 | 16:07 | 22.6 | 304 | 7.47 | 0.72 | 5.3784 |
| 2/3/21 | 16:06 | 22.5 | 307.3 | 9.03 | 0.719 | 6.49257 |
| 2/3/21 | 16:06 | 22.6 | 308.5 | 10.41 | 0.713 | 7.42233 |
| 2/3/21 | 16:05 | 22.4 | 311.9 | 11.74 | 0.705 | 8.2767 |
| 2/3/21 | 16:04 | 22.2 | 315.6 | 12.89 | 0.688 | 8.86832 |
| 2/3/21 | 16:04 | 22.1 | 316.8 | 14.04 | 0.657 | 9.22428 |
| 3/3/21 | 14:56 | 37.6 | 559.1 | 2.612 | 1.392 | 3.635904 |
| 3/3/21 | 14:56 | 37.8 | 559.1 | 0.248 | 1.418 | 0.351664 |
| 3/3/21 | 14:55 | 37.6 | 559.7 | 5.482 | 1.393 | 7.636426 |
| 3/3/21 | 14:53 | 38.6 | 561.8 | 7.66 | 1.337 | 10.24142 |
| 3/3/21 | 14:52 | 39.9 | 567.6 | 11.88 | 1.162 | 13.80456 |
| 3/3/21 | 14:52 | 39.6 | 567.6 | 10.17 | 1.254 | 12.75318 |
| 3/3/21 | 14:48 | 40.6 | 576.8 | 15.81 | 0.755 | 11.93655 |
| 3/3/21 | 14:50 | 39.8 | 576.8 | 14.98 | 0.89 | 13.3322 |
| 3/3/21 | 14:50 | 40.6 | 576.8 | 14.26 | 0.973 | 13.87498 |
| 3/3/21 | 14:51 | 40.2 | 576.8 | 13.38 | 1.068 | 14.28984 |
| 3/3/21 | 14:49 | 40.2 | 582.3 | 15.42 | 0.811 | 12.50562 |
| 9/3/21 | 15:25 | 46.3 | 707.1 | 18.98 | 0 | 0 |
| 9/3/21 | 15:24 | 46.1 | 710 | 17.78 | 0.446 | 7.92988 |
| 3/3/21 | 14:51 | 40.2 | 576.8 | 13.38 | 1.068 | 14.28984 |
| 3/3/21 | 14:49 | 40.2 | 582.3 | 15.42 | 0.811 | 12.50562 |
| 9/3/21 | 15:25 | 46.3 | 707.1 | 18.98 | 0 | 0 |
| 9/3/21 | 15:24 | 46.1 | 710 | 17.78 | 0.446 | 7.92988 |
| 9/3/21 | 15:20 | 45.2 | 723 | 16.84 | 0.735 | 12.3774 |
| 9/3/21 | 15:20 | 45.4 | 723 | 17.05 | 0.677 | 11.54285 |
| 9/3/21 | 15:20 | 45.7 | 723 | 17.23 | 0.625 | 10.76875 |
| 9/3/21 | 15:17 | 44 | 724 | 16.32 | 0.874 | 14.26368 |
| 9/3/21 | 15:17 | 44.1 | 724.2 | 15.92 | 0.958 | 15.25136 |
| 9/3/21 | 15:16 | 45.5 | 724.5 | 15.43 | 1.05 | 16.2015 |
| 9/3/21 | 15:19 | 44.3 | 725.7 | 17.94 | 0.429 | 7.69626 |

STUDY ON PARTIALLY SHADED CONDITIONS REGULATORS FOR PV BASED ELECTRICALLY POWERED VEHICLES

| | | | | | | |
|--------|-------|------|-------|-------|-------|----------|
| 9/3/21 | 15:18 | 43.9 | 726 | 16.62 | 0.807 | 13.41234 |
| 9/3/21 | 15:15 | 45.1 | 730.3 | 10.43 | 1.676 | 17.48068 |
| 9/3/21 | 15:15 | 46 | 730.3 | 12.68 | 1.474 | 18.69032 |
| 9/3/21 | 15:15 | 46.2 | 730.3 | 13.78 | 1.326 | 18.27228 |
| 9/3/21 | 15:13 | 45.8 | 732.7 | 0.392 | 1.9 | 0.7448 |
| 9/3/21 | 15:14 | 45.8 | 736.1 | 3.146 | 1.872 | 5.889312 |
| 9/3/21 | 15:14 | 45 | 736.1 | 7.03 | 1.824 | 12.82272 |
| 8/3/21 | 16:17 | 30 | 741 | 20 | 0 | 0 |
| 8/3/21 | 16:16 | 30.3 | 747.7 | 18.83 | 0.467 | 8.79361 |
| 8/3/21 | 16:16 | 30.8 | 747.7 | 18.88 | 0.448 | 8.45824 |
| 8/3/21 | 16:13 | 29.3 | 748.6 | 18.55 | 0.641 | 11.89055 |
| 8/3/21 | 16:16 | 29.4 | 749.2 | 18.78 | 0.491 | 9.22098 |
| 8/3/21 | 16:15 | 29.9 | 751.3 | 18.73 | 0.52 | 9.7396 |
| 8/3/21 | 16:14 | 28.8 | 756.2 | 18.62 | 0.599 | 11.15338 |
| 8/3/21 | 16:14 | 30.3 | 758.4 | 18.67 | 0.552 | 10.30584 |

For an array composed of panels A and D in series, being A under an irradiance of 100W/m^2 and D under an irradiance of 700W/m^2 the experimental results are the following ones:

Table A.5: data recorded for array A-D under PSC

| DATE | TIME | IRRADIANCE ON PANEL D (W/m ²) | VOLTAGE (V) | CURRENT (A) | POWER (W) |
|---------|-------|---|-------------|-------------|-----------|
| 22/6/21 | 10:54 | 722.4 | 15.27 | 0.015 | 0.22905 |
| 22/6/21 | 11:36 | 792.2 | 15.08 | 0.015 | 0.2262 |
| 22/6/21 | 10:55 | 715.9 | 14.78 | 0.017 | 0.25126 |
| 22/6/21 | 11:37 | 803.5 | 14.54 | 0.017 | 0.24718 |
| 22/6/21 | 10:55 | 715.9 | 14.08 | 0.123 | 1.73184 |
| 22/6/21 | 10:56 | 713.8 | 13.64 | 0.158 | 2.15512 |
| 22/6/21 | 10:56 | 713.8 | 12.95 | 0.284 | 3.6778 |
| 22/6/21 | 10:57 | 711.7 | 12.38 | 0.298 | 3.68924 |
| 22/6/21 | 10:57 | 711.7 | 11.98 | 0.327 | 3.91746 |
| 22/6/21 | 10:58 | 717.2 | 11.45 | 0.332 | 3.8014 |
| 22/6/21 | 10:58 | 717.2 | 10.58 | 0.368 | 3.89344 |
| 22/6/21 | 11:09 | 764.8 | 10.22 | 0.489 | 4.99758 |
| 22/6/21 | 11:35 | 798.3 | 9.95 | 0.366 | 3.6417 |

STUDY ON PARTIALLY SHADED CONDITIONS REGULATORS FOR PV BASED ELECTRICALLY POWERED VEHICLES

| | | | | | |
|---------|-------|-------|-------|-------|----------|
| 22/6/21 | 11:09 | 764.8 | 9.57 | 0.547 | 5.23479 |
| 22/6/21 | 11:12 | 747.4 | 8 | 0.745 | 5.96 |
| 22/6/21 | 11:13 | 751 | 7.67 | 0.794 | 6.08998 |
| 22/6/21 | 11:13 | 751 | 7.13 | 0.864 | 6.16032 |
| 22/6/21 | 11:13 | 751 | 6.6 | 0.924 | 6.0984 |
| 22/6/21 | 11:14 | 747.7 | 5.8 | 1.099 | 6.3742 |
| 22/6/21 | 11:14 | 747.7 | 5.24 | 1.132 | 5.93168 |
| 22/6/21 | 11:15 | 752.9 | 4.42 | 1.153 | 5.09626 |
| 22/6/21 | 11:15 | 752.9 | 3.52 | 1.188 | 4.18176 |
| 22/6/21 | 11:15 | 752.9 | 2.22 | 1.23 | 2.7306 |
| 22/6/21 | 11:16 | 752.3 | 1.64 | 1.3 | 2.132 |
| 22/6/21 | 11:17 | 749.8 | 0.677 | 1.3 | 0.8801 |
| 22/6/21 | 11:18 | 770.6 | 0.246 | 1.33 | 0.32718 |
| 22/6/21 | 11:18 | 770.6 | 0.188 | 1.376 | 0.258688 |

APPENDIX 2

MEASUREMENT OF THE VOLTAGE AND CURRENT AT THE INPUT AND OUTPUTS OF THE COMMERCIAL LOAD REGULATOR

Table A.6: Measurements from the commercial load regulator

| | CONF 1 | CONF 2 | CONF 3 | CONF 4 |
|--------------------------------|---------------|---------------|---------------|---------------|
| DATE | 24-mar | 24-mar | 24-mar | 24-mar |
| TIME | 10:30 | 10:43 | 10:55 | 11:13 |
| T _{AMB} (°C) | 16.6 | 16.1 | 16.3 | 16.4 |
| IRRADIANCE (W/m ²) | 874.3 | 880.1 | 888.4 | 854.8 |
| T _{PANEL A} (°C) | 41.5 | 37.6 | 43.5 | 39.5 |
| T _{PANEL B} (°C) | 42.7 | 37.2 | 43.7 | 42.1 |
| T _{PANEL C} (°C) | 42.2 | 40.4 | 42 | - |
| T _{PANEL D} (°C) | 42.3 | 39.4 | 41.2 | - |
| V _{PANELS} (V) | 26.43 | 25.16 | 24.47 | 25.54 |
| V _{BATTERIES} (V) | 25.91 | 24.70 | 24.17 | 25.08 |
| V _{LOAD} (V) | 25.78 | 24.59 | 23.97 | 24.93 |
| I _{PANELS} (A) | 4.112 | 2.401 | 0.696 | 2.178 |
| I _{BATTERIES} (A) | 0.384 | -1.315 | -2.932 | -1.468 |
| I _{LOAD} (A) | 3.831 | 3.736 | 3.614 | 3.698 |

*Current from the batteries is positive when they receive current from the PV-array and negative in the cases where they feed the load.

APPENDIX 3

CODE FOR THE BOOST CONVERTER FEEDING A LOAD WITH CONSTANT VOLTAGE BY PANELS UNDER CONSTANT IRRADIANCE CONDITIONS

```
function D=OutputTracking(Vo)
deltaD=0.001;
persistent iteration prevD prevVo K ReachSetpoint
if isempty(iteration)
    ReachSetpoint=0;
    D=0.8;
    iteration=1;
    K=1;
    prevD=D;
    prevVo=Vo;
else
    iteration=iteration+1;
    D=prevD;
end
if mod(iteration,5000)==0
    if Vo<24,
        if prevVo<Vo && D>0.1,
            D=D-deltaD;
        else
            if prevVo>Vo && D<.9 && ReachSetpoint==0,
                ReachSetpoint=1;
                D=D+deltaD;
            end
        end
    end
    else
        K=K*1;

        if prevVo>Vo && D>0.1,
            D=D+deltaD*K;
        else
            if prevVo<Vo && D<.9,
                D=D+deltaD*K;
            end
        end
    end
    prevVo=Vo;
end
prevD=D;
```

APPENDIX 4

CODE FOR THE PERTURBATION & OBSERVATION MPPT ALGORITHM

```
function D = PandO(Vpv, Ipv)
sample=10^-6; % PWM block sampling time
Ts=.05; %Micro sampling time
fs=Ts/sample;

persistent Dprev Pprev Vprev iteration

if isempty(iteration),
    D=0.95; %initial value for D
    iteration=1;
    Dprev=D;
    Vprev=10;
    Pprev=20;
else
    iteration=iteration+1;
    D=Dprev;
end
if mod(iteration, fs)==0
    deltaD=0.01;
    Ppv=Vpv*Ipv;
    % INcrease/decrease D based on conditions:
    if (Ppv-Pprev)~=0
        if (Ppv-Pprev)>0
            if (Vpv-Vprev)>0
                D=Dprev-deltaD;
            else
                D=Dprev+deltaD;
            end
        else
            if (Vpv-Vprev)>0
                D=Dprev+deltaD;
            else
                D=Dprev-deltaD;
            end
        end
    else
        D=Dprev;
    end
    Dprev=D;
    Vprev=Vpv;
    Pprev=Ppv;
end
```


APPENDIX 5

CODE FOR THE DUTY SWEEPING ALGORITHM

```

function [ D,deltaP]=MPPT(Vpv,Ipv)
% variables definitions
deltaD=0.01;
D0=0.9+deltaD;
sample=10^-6; %PWM block sampling time
Ts=.050; % micro sampling time
fs=Ts/sample; %our sampling frequency
N_samples=50; %the number of samples used to record the load curve
iter_limit=N_samples*Ts/(sample); %specify the limit
persistent vectP vectV vectD vectI prevPp prevVp prevIp iteration n
prevD sweeping iter
%Pnom=%POTENCIA NOMINAL
if isempty(iteration),
    iter=0;
    deltaP=0
    D=D0;%initial value for D
    iteration=1;
    vectP=ones(N_samples,1);
    vectV=ones(N_samples,1);
    vectD=ones(N_samples,1);
    vectI=ones(N_samples,1);
    n=1;
    prevD=D;
    prevIp=Ipv;
    prevPp=Vpv*Ipv;
    prevVp=Vpv;
    sweeping=1;
else
    iteration=iteration+1;
    iter=iter+1;
    D=prevD;
end
if sweeping,
    deltaP=0;
if iteration<=iter_limit
    if mod(iteration,fs)==0
        D=prevD-deltaD;
        Ppv=Vpv*Ipv;
        vectP(n)=[Ppv];
        vectV(n)=[Vpv];
        vectD(n)=[D];
        vectI(n)=[Ipv];
        n=n+1;
    end
    if n==N_samples+1,
        [Pmax,posPmax]=max(vectP);
        V_pmax= vectV(posPmax);
        D_pmax= vectD(posPmax);
        I_pmax= vectI(posPmax);
        D=D_pmax;
        Vpv=V_pmax;
        Ipv=I_pmax;

        sweeping=0;
        n=1;
    end
end

```

STUDY ON PARTIALLY SHADED CONDITIONS REGULATORS FOR PV BASED ELECTRICALLY POWERED VEHICLES

```
        iteration=0; %%%reset counter to 0
    end
end
else
    deltaP=0;
    if iter==745000
        iter;
    end
    if mod(iteration,fs)==0,
        [D, sweeping, deltaP]=PandO(Vpv,Ipv, prevD,prevVp,prevPp);
        if sweeping,
            iteration=0;
            D=D0-deltaD;
        end
    else
        Vpv=prevVp;
        Ipv=prevIp;
    end
end
prevD=D;
prevPp=Vpv*Ipv;
prevIp=Ipv;
prevVp=Vpv;
end
function [D, sweeping, deltaP] = PandO(Vpv,Ipv, D, Vp, Pp)
    Dprev=D;
    Vprev=Vp;
    Pprev=Pp;
    deltaD=.001;
    % Calculate measured power:
    Ppv=Vpv*Ipv;
    % INcrease/decrease D based on conditions:
    deltaP=abs(Ppv-Pprev);
    disp(deltaP/Pprev)
    if deltaP/Pprev>.1 && Pprev>Ppv,%if variation is higher than 10%
    sweeping starts
        sweeping=1;
    else
        sweeping=0;
    end
    if deltaP~=0
        if (Ppv-Pprev)>0
            if (Vpv-Vprev)>0
                D=Dprev-deltaD;
            else
                D=Dprev+deltaD;
            end
        else
            if (Vpv-Vprev)>0
                D=Dprev+deltaD;
            else
                D=Dprev-deltaD;
            end
        end
    end
    else
        D=Dprev;
    end
end
```

APPENDIX 6

PANEL A PARAMETERS AND I-V CURVE WITH $T_{AMB}=24^{\circ}C$

Table A.7: data recorded for panel A at high temperature

| PANEL A | | | | | | | |
|---------|-------|-----------|-----------|-------------------|-------------|-------------|-----------|
| DATE | TIME | Tsup (°C) | Tamb (°C) | IRRADIANCE (W/m2) | VOLTAGE (V) | CURRENT (A) | POWER (W) |
| 6/5/21 | 12:26 | 37.6 | 24.546488 | 894.8 | 0.163 | 2.146 | 0.349798 |
| 7/5/21 | 12:27 | 37.5 | 24.643256 | 896.3 | 3.275 | 2.12 | 6.943 |
| 8/5/21 | 12:27 | 37.9 | 24.643256 | 896.3 | 7.59 | 2.105 | 15.97695 |
| 9/5/21 | 12:28 | 38 | 24.643426 | 895.6 | 11.47 | 2.037 | 23.36439 |
| 10/5/21 | 12:29 | 38.2 | 24.786446 | 895.2 | 14.02 | 1.753 | 24.57706 |
| 11/5/21 | 12:30 | 38.3 | 24.919776 | 895.4 | 15.24 | 1.532 | 23.34768 |
| 12/5/21 | 12:30 | 39.1 | 24.919776 | 895.4 | 16.4 | 1.323 | 21.6972 |
| 13/5/21 | 12:31 | 39.5 | 24.896302 | 895.1 | 16.87 | 1.161 | 19.58607 |
| 14/5/21 | 12:32 | 39.3 | 24.976426 | 898.1 | 17.17 | 1.029 | 17.66793 |
| 15/5/21 | 12:32 | 39.6 | 24.976426 | 898.1 | 17.4 | 0.93 | 16.182 |
| 16/5/21 | 12:33 | 39.5 | 25.095258 | 897.2 | 17.6 | 0.838 | 14.7488 |
| 17/5/21 | 12:35 | 40.7 | 24.948448 | 902.7 | 17.62 | 0.739 | 13.02118 |
| 18/5/21 | 12:35 | 40.3 | 24.94845 | 902.7 | 17.75 | 0.721 | 12.79775 |
| 19/5/21 | 12:36 | 42.4 | 24.901868 | 904.5 | 17.83 | 0.67 | 11.9461 |
| 20/5/21 | 12:37 | 42.2 | 24.8579 | 904.5 | 17.9 | 0.618 | 11.0622 |
| 21/5/21 | 12:37 | 42.7 | 24.8579 | 904.5 | 17.94 | 0.58 | 10.4052 |
| 22/5/21 | 12:37 | 42.8 | 24.8579 | 904.5 | 17.99 | 0.539 | 9.69661 |
| 23/5/21 | 12:38 | 42.6 | 24.796884 | 906.1 | 18.04 | 0.57 | 10.2828 |
| 24/5/21 | 12:39 | 41.6 | 24.717254 | 911.3 | 18.06 | 0.481 | 8.68686 |
| 25/5/21 | 12:39 | 41.8 | 24.71725 | 911.3 | 18.1 | 0.454 | 8.2174 |
| 26/5/21 | 12:40 | 42.5 | 24.634422 | 908.8 | 18.09 | 0.433 | 7.83297 |
| 27/5/21 | 12:43 | 38.7 | 24.275282 | 917.7 | 18.8 | 0.1 | 1.88 |
| 28/5/21 | 12:44 | 38.4 | 24.164026 | 914.6 | 18.82 | 0.099 | 1.86318 |
| 29/5/21 | 12:45 | 37.3 | 24.078394 | 916.4 | 18.84 | 0.008 | 0.15072 |

| | | | | | | | |
|---------|-------|------|----------|-------|-------|-------|---|
| 30/5/21 | 12:48 | 37.8 | 23.93439 | 919.5 | 18.85 | 0.002 | 0 |
| 31/5/21 | 12:48 | 37.8 | 23.93439 | 921 | 19.03 | 0 | 0 |

APPENDIX 7

ESTIMATED EQUATIONS FOR THE I-V CURVES

Using Excel's tool available to estimate the equation of a curve, the different I-V equations of each panel have been approximated.

PANEL A

- $I_{rr}=900 \text{ W/m}^2$:

$$I = -1E - 04V^4 + 0.0026V^3 - 0.0233V^2 + 0.0601V + 2.4063$$

- $I_{rr}=650 \text{ W/m}^2$:

$$I = -3E - 05V^4 + 0.0003V^3 + 0.0029V^2 - 0.0229V + 1.5068$$

- $I_{rr}=400 \text{ W/m}^2$:

$$I = -1E - 05V^4 + 0.0002V^3 - 0.0005V^2 - 0.0016V + 1.1193$$

- $I_{rr}=100 \text{ W/m}^2$:

$$I = -0.0005V^3 + 0.0144V^2 - 0.0978V + 0.4576$$

PANEL B

- $I_{rr}=820 \text{ W/m}^2$:

$$I = -9E - 05V^4 + 0.0022V^3 - 0.0184V^2 + 0.0513V + 2.0493$$

- $I_{rr}=600 \text{ W/m}^2$:

$$I = -2E - 05V^4 - 0.0002V^3 + 0.0118V^2 - 0.1086V + 1.6793$$

- $I_{rr}=350 \text{ W/m}^2$:

$$I = -2E - 05V^4 + 0.0005V^3 - 0.0058V^2 + 0.0399V + 0.8514$$

- $I_{rr}=100 \text{ W/m}^2$:

$$I = -2E - 05V^4 + 0.0005V^3 - 0.0043V^2 + 0.0112V + 0.2788$$

PANEL C

- $I_{rr}=740 \text{ W/m}^2$:

$$I = -1E - 05V^4 - 0.0003V^3 + 0.0082V^2 - 0.063V + 2.0974$$

- $I_{rr}=500-600 \text{ W/m}^2$:

$$I = -7E - 06V^5 + 0.0002V^4 - 0.0032V^3 + 0.0153V^2 - 0.0327V + 1.3085$$

- $I_{rr}=85 \text{ W/m}^2$:

$$I = -5E - 06V^4 + 0.0001V^3 - 0.0006V^2 - 0.0015V + 0.2639$$

PANEL D

- $I_{rr}=740 \text{ W/m}^2$:

$$I = 2E - 05V^4 - 0.0009V^3 + 0.0073V^2 - 0.021V + 1.9016$$

- $I_{rr}=500-600 \text{ W/m}^2$:

$$I = -4E - 05V^4 + 0.001V^3 - 0.0106V^2 + 0.0314V + 1.3985$$

- $I_{rr}=300 \text{ W/m}^2$:

Not available as curve could not be completed experimentally.

- $I_{rr}=80 \text{ W/m}^2$:

Not available as curve could not be completed experimentally.

The next figures show the approximation curves over the real curves:

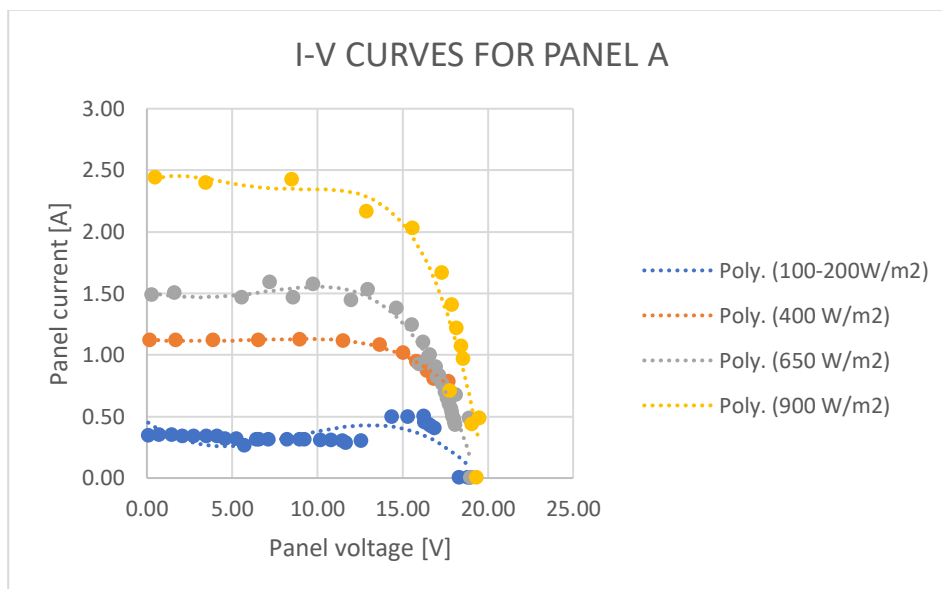


Figure A.1: Approximated I-V curves for panel A

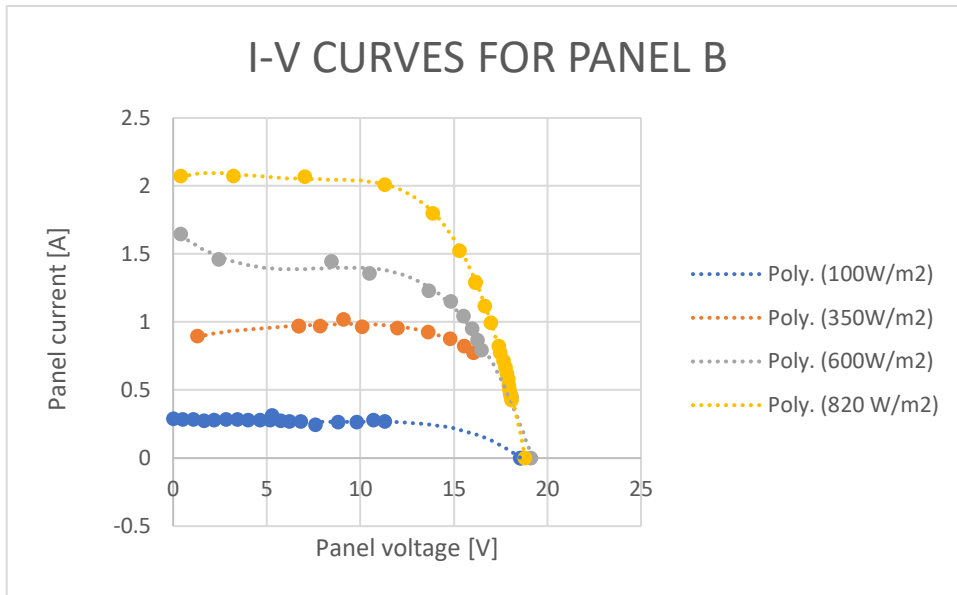


Figure A.2: Approximated I-V curves for panel B

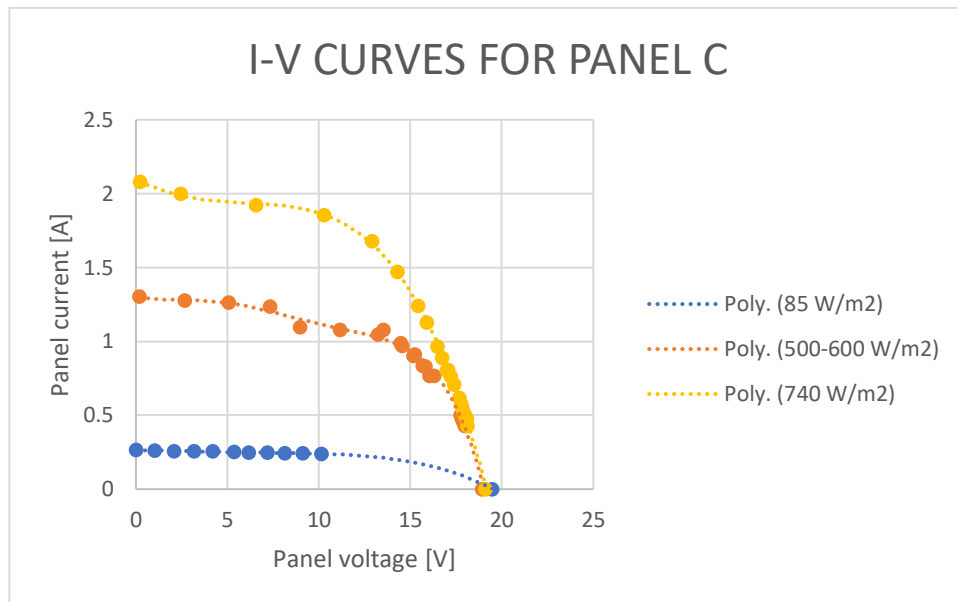


Figure A.3: Approximated I-V curves for panel C

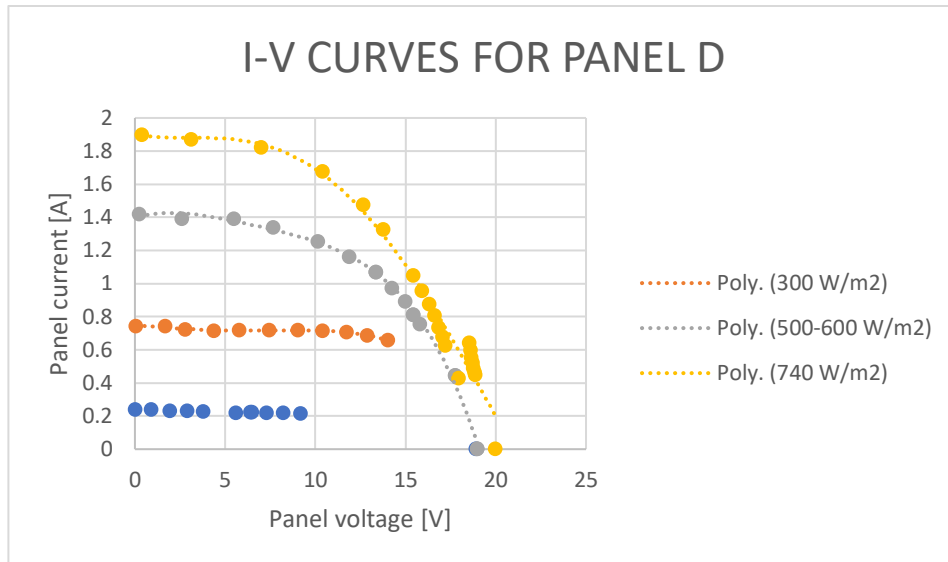


Figure A.4: Approximated I-V curves for panel D

LINEAR RELATION BETWEEN SHORTCIRCUIT CURRENT AND IRRADIANCE

As stated in [5], the short-circuit current (I_{sc}) is proportional to irradiance. Therefore, it is interesting to contrast the relation of the I_{sc} of the panels under study and each irradiance curve to prove that this relation holds and show the value of the electrical current as a function of the irradiance:

Table A.8: Irradiance-Current ratio for panel A

| PANEL A | | |
|---------|--------------------------------|------------------------------|
| Isc (A) | IRRADIANCE (W/m ²) | RATIO [(Am ²)/W] |
| 2.44 | 897 | 1/367.62 |
| 1.5 | 524 | 1/349.33 |
| 1.12 | 400 | 1/357.14 |
| 0.35 | 110 | 1/314.28 |

Table A.9: Irradiance-Current ratio for panel B

| PANEL B | | |
|---------|--------------------------------|------------------------------|
| Isc (A) | IRRADIANCE (W/m ²) | RATIO [(Am ²)/W] |

| | | |
|-------|-------|----------|
| 2.073 | 847.8 | 1/408.97 |
| 1.461 | 610.4 | 1/417.79 |
| 0.962 | 392.2 | 1/407.69 |
| 0.288 | 100 | 1/347.22 |

Table A.10: Irradiance-Current ratio for panel C

| PANEL C | | |
|---------|--------------------------------|------------------------------|
| Isc (A) | IRRADIANCE (W/m ²) | RATIO [(Am ²)/W] |
| 2.08 | 784.6 | 1/377.21 |
| 1.461 | 610.4 | 1/417.79 |
| 0.264 | 86.4 | 1/327.27 |

Table A.11: Irradiance-Current ratio for panel D

| PANEL D | | |
|---------|--------------------------------|------------------------------|
| Isc (A) | IRRADIANCE (W/m ²) | RATIO [(Am ²)/W] |
| 1.9 | 732.7 | 1/385.63 |
| 1.418 | 559.1 | 1/394.29 |
| 0.744 | 296.9 | 1/399.06 |
| 0.24 | 82.7 | 1/344.58 |

Except for the last value of each table, when the panels are facing backwards to the Sun, irradiation is too low, in general, the direct proportionality between irradiance and short-circuit current is clearly seen. The difference of this last case may arise because the irradiance received by the panels in that situation is totally diffuse and direct irradiance is non-existing. The pyranometer measures the total and the diffuse irradiance, being the total (presented in the tables) the sum of the direct and the diffuse irradiance. These panels do not receive any direct irradiance as it is the one that travels in a straight line from the sun the panel and in this case the total irradiance coincides with the diffuse.

For panel A, the proportionality ratio diverges slightly from the rest, it is approximately 12% higher than for panels B, C and D. It probably occurs due to two

reasons, because the specifications of this panel may be slightly better than the ones of the rest or due to the inaccuracy at the measurement of the short-circuit currents of this P-V panel.

For each of the P-V panels, the proportional ratio $I_{sc}/Irradiance$ is estimated as it follows:

$$\begin{aligned} \text{PANEL A} &\rightarrow I_{sc}/Irradiance = 1/358.03 \frac{W}{A \cdot m^2} \\ \text{PANEL B} &\rightarrow I_{sc}/Irradiance = 1/411.48 \frac{W}{A \cdot m^2} \\ \text{PANEL C} &\rightarrow I_{sc}/Irradiance = 1/397.50 \frac{W}{A \cdot m^2} \\ \text{PANEL D} &\rightarrow I_{sc}/Irradiance = 1/392.99 \frac{W}{A \cdot m^2} \end{aligned}$$

LINEAR FACTOR BETWEEN CURVES AND ESTIMATION OF CURVES FOR DIFFERENT IRRADIANCE VALUES

In order to estimate the short-circuit current (I_{sc}) corresponding to other irradiance curves, the relation among the recording data is studied. By obtaining a factor that relates the existing I-V curves, short-circuit current at any irradiance situation can be estimated.

To see if the forementioned factor exists, the relation between each pair of irradiation curves and their respective I_{sc} is calculated.

The following tables show the ratio between I_{sc} and between irradiances of each pair of curves from the tables in previous section:

Table A.12: Linear factor between currents and irradiances for panel A

| PANEL A | | |
|--|---------------------|---------------|
| | I_{sc_i}/I_{sc_j} | Irr_i/Irr_j |
| $i=897 \text{ W/m}^2, j=524 \text{ W/m}^2$ | 1.62 | 1.71 |
| $i=897 \text{ W/m}^2, j=400 \text{ W/m}^2$ | 2.18 | 2.24 |
| $i=897 \text{ W/m}^2, j=100 \text{ W/m}^2$ | 6.97 | 8.15 |
| $i=524 \text{ W/m}^2, j=400 \text{ W/m}^2$ | 1.34 | 1.31 |

| | | |
|--|------|------|
| $i=524 \text{ W/m}^2, j=100 \text{ W/m}^2$ | 4.29 | 4.76 |
| $i=400 \text{ W/m}^2, j=100 \text{ W/m}^2$ | 3.20 | 3.64 |

Table A.13: Linear factor between currents and irradiances for panel B

| PANEL B | | |
|--|--|--|
| | Isc_i/Isc_j | Irr_i/Irr_j |
| $i= 848 \text{ W/m}^2, j= 610.4 \text{ W/m}^2$ | 1.42 | 1.39 |
| $i=848 \text{ W/m}^2, j=392 \text{ W/m}^2$ | 2.15 | 2.16 |
| $i=848 \text{ W/m}^2, j=100 \text{ W/m}^2$ | 7.20 | 8.47 |
| $i=610.4 \text{ W/m}^2, j=392 \text{ W/m}^2$ | 1.512 | 1.55 |
| $i=610.4 \text{ W/m}^2, j=100 \text{ W/m}^2$ | 5.07 | 6.10 |
| $i=392 \text{ W/m}^2, j= 100 \text{ W/m}^2$ | 3.340 | 3.92 |

Table A.14: Linear factor between currents and irradiances for panel C

| PANEL C | | |
|--|--|--|
| | Isc_i/Isc_j | Irr_i/Irr_j |
| $i=784.6 \text{ W/m}^2, j=610 \text{ W/m}^2$ | 1.42 | 1.29 |
| $i=784.6 \text{ W/m}^2, j=86 \text{ W/m}^2$ | 7.88 | 9.08 |
| $i=610 \text{ W/m}^2, j=86 \text{ W/m}^2$ | 5.53 | 7.06 |

Table A.15: Linear factor between currents and irradiances for panel D

| PANEL D | | |
|--|--|--|
| | Isc_i/Isc_j | Irr_i/Irr_j |
| $i= 732.7, \text{ W/m}^2 j= 559.1 \text{ W/m}^2$ | 1.34 | 1.31 |
| $i=732.7, \text{ W/m}^2, j=296.9 \text{ W/m}^2$ | 2.55 | 2.467 |
| $i=732.7, \text{ W/m}^2, j=82.7 \text{ W/m}^2$ | 7.92 | 8.86 |
| $i=559.1 \text{ W/m}^2, j=296.9 \text{ W/m}^2$ | 1.91 | 1.88 |
| $i=559.1 \text{ W/m}^2, j=82.7 \text{ W/m}^2$ | 5.91 | 6.76 |
| $i=296.9 \text{ W/m}^2, j=82.7 \text{ W/m}^2$ | 3.1 | 3.59 |

After comparing the rates of the four P-V panels, it can be concluded that the following relation holds quite accurately:

$$\frac{I_{sc_i}}{I_{sc_j}} \approx \frac{Irr_i}{Irr_j} \quad (eq. 18)$$

Consequently, the following equation can be used to estimate the short-circuit current corresponding to a certain irradiance having the I_{sc} given for another value of irradiance:

$$I_{sc_i} = Irr_i \cdot \frac{I_{sc_j}}{Irr_j} \quad (eq. 19)$$

Below, the short-circuit current corresponding to some irradiances is estimated with eq.17:

PANEL C

For an irradiance of 400 W/m^2 , the estimated short-circuit current is the following:

$$I_{sc_{400}} = 400 \cdot \frac{I_{sc_j}}{Irr_j} = 400 \frac{\text{W}}{\text{m}^2} \cdot \frac{2.08 \text{ A}}{784.6 \text{ W/m}^2} = 1.11 \text{ A}$$

PANEL D

For an irradiance of 850 W/m^2 , the estimated short-circuit current is the following:

$$I_{sc_{850}} = 850 \cdot \frac{I_{sc_j}}{Irr_j} = 850 \frac{\text{W}}{\text{m}^2} \cdot \frac{1.9 \text{ A}}{732.7 \text{ W/m}^2} = 2.20 \text{ A}$$

These values estimated for panels C and D are similar to the corresponding I_{sc} from panels A and B in similar circumstances. Consequently, it can be considered a correct estimation in order to define the curves corresponding to different irradiance values.